Numerical Algorithms
https://doi.org/10.1007/s11075-024-01987-6

RESEARCH

High accuracy two-level compact implicit method in exponential form for 2D fourth order quasi-linear parabolic equations

Divya Sharma[1] · Kajal Mittal[2] · Deepti Kaur[3] · Rajendra K. Ray[2] · R.K. Mohanty[1]

Received: 2 July 2024 / Accepted: 17 November 2024

Abstract
In this study, we develop a nine-point compact difference scheme in exponential form to solve two-dimensional second-order quasi-linear parabolic equations with Dirichlet boundary conditions. The proposed two-level implicit difference method is fourth-order accurate in space and second-order accurate in time. Further, the method is extended to a vectorized form for solving systems of quasi-linear parabolic equations and applied to fourth-order parabolic equations without the need for fictitious nodes to incorporate the boundary conditions. Additionally, an operator splitting technique is employed to solve the 2D linear model equation and is shown to be unconditionally stable. Numerical experiments are conducted on several benchmark problems, including the viscous unsteady Burgers' equation, time-dependent Navier-Stokes equations of motion, Taylor-Vortex problem, Extended Fisher-Kolmogorov equation, and Kuramoto-Sivashinsky equation. Numerical results demonstrate that the findings acquired not only accord well with the exact solutions but are also competent with solutions derived from previous research investigations.

✉ Rajendra K. Ray
rajendra@iitmandi.ac.in

Divya Sharma
udivya93@gmail.com

Kajal Mittal
kajalmittal90@gmail.com

Deepti Kaur
deeptikaur@ms.du.ac.in

R.K. Mohanty
rmohanty@sau.ac.in

1 Department of Mathematics, South Asian University, New Delhi, India

2 School of Mathematical and Statistical Sciences, IIT Mandi, Himachal Pradesh, India

3 Department of Mathematics, Mata Sundri College for Women, University of Delhi, New Delhi, India

Published online: 04 December 2024

Keywords Quasi-linear parabolic equation · High-order compact implicit method · Extended Fisher-Kolmogorov equation · Navier-Stokes equations · Burgers' equation · Kuramoto-Sivashinsky equation

Mathematics Subject Classification (2010) 65M06 · 65M12 · 65M22

1 Introduction

Consider the two-dimensional quasi-linear second-order parabolic partial differential equation (PPDE) having the structure:

$$A\left(x,y,t\right)\frac{\partial^2 u}{\partial x^2}+C\left(x,y,t\right)\frac{\partial^2 u}{\partial y^2}=f\left(x,y,t,u,u_x,u_y,u_t\right),\quad (x,y,t)\in\Omega_2 \tag{1.1}$$

with the following Dirichlet boundary conditions:

$$u\left(0,y,t\right)=f_0\left(y,t\right),\quad u\left(a,y,t\right)=f_1\left(y,t\right),\quad 0\le y\le a,\quad t>0, \tag{1.2}$$
$$u\left(x,0,t\right)=g_0\left(x,t\right),\quad u\left(x,a,t\right)=g_1\left(x,t\right),\quad 0\le x\le a,\quad t>0, \tag{1.3}$$

and the initial condition:

$$u\left(x,y,0\right)=u_0\left(x,y\right),\quad 0\le x,y\le a, \tag{1.4}$$

where the solution space $\Omega_2=\{(x,y,t):0\le x,y\le a, 0<t<T\}$, a is a real number and T is the final time. We assume that $u(x,y,t)\in C^{(6,6,2)}(\Omega_2)$, $A(x,y,t)\in C^{(4,4,2)}(\Omega_2)$, $C(x,y,t)\in C^{(4,4,2)}(\Omega_2)$, and f_0, f_1, g_0, g_1 and u_0 are adequately smooth functions. Also, we suppose that there is only ever one continuous function to the initial-boundary value problem (IBVP) (1.1)-(1.4) in the solution domain Ω_2. The above equation models many real-life phenomena and arises in a variety of mathematical models of technical challenges in the physical sciences and engineering, including fluid flow, mass and heat transfer, chemical reactions, and many more [6, 16, 45, 46]. The class of IBVPs (1.1)-(1.4) admits, in specific, the Burgers' and Navier-Stokes equations (NSEs) that demonstrate the presence of the conservation rules for mass, energy, and momentum and explain fluid motion and turbulent flow [6, 19]. These equations are the primary foundation of computational fluid dynamics.

Analytical solutions to these equations seem overly complicated and impractical in most situations. Even in the simplest of cases, closed-form solutions to PPDEs are rare and only applicable to a small subset of the problems. The numerical solution of IBVPs (1.1)-(1.4) has drawn the interest of several scholars in the past, leading to the development of diverse approaches like explicit and implicit difference schemes. However, developing high-order, accurate, and computationally economical approximation algorithms for time-dependent problems with changing coefficients remains a formidable challenge. In order to solve the time-dependent NSEs for an incompressible fluid, Chorin [6] made the earliest contribution in this field by using a finite difference method of order two. Ghia et al. [16] obtained fine mesh solutions for high Reynolds number flow using the coupled implicit and multigrid methods for the computation of the 2D incompressible NSEs. Distinguished work has been done by Li et al. [28], Spotz and Carey [45], and Weinan and Liu [48] for the construction and advancement of high-order compact methods with high-accuracy boundary treatment for the stream-function vorticity equations for NSEs. Tafti [47] investigated the numerical treatment of the unsteady incompressible NSEs on a collocated grid. Hirsh [19] developed and applied the compact fourth-order differencing method proposed by Kreiss for the computation of Burgers' equation. Fletcher [15] applied a second-order approach based on finite difference for the 2D Burgers' equation for fluid flows. Later, Mohanty and Jain [33] derived a two-level compact implicit difference technique for treating the general two-space non-linear PPDE with non-constant coefficients numerically. For the incompressible NSEs, Strikwerda [46] presented finite difference methods on the basis of two different spatial differencing approaches, one of which is accurate to fourth order and another of which is correct to the sixth order. Afterwards, Yanwen et al. [49] demonstrated the finite difference approach for the incompressible NSEs and introduced a close approximation of convection terms with an upwind compact difference that is accurate to the fifth order, the viscous terms with a compact difference approximation accurate to the sixth order for symmetrical flows, continuity equation and the pressure gradient in momentum equations with a difference approximation accurate to the fourth order on a cell-centered mesh, and so on.

A conditionally stable explicit finite difference technique for handling advective elements in the two-dimensional equation of unstable scalar transport was first proposed by Balzano [5], and later it was applied for solving the conservative version of the depth-averaged (DA) transport equation. Over the years, many highly accurate, compact techniques have been developed for different fluid flow models. Further, Meitz and Fasel [30] used the Fourier collocation approach to obtain compact difference discretization for the incompressible, unsteady NSEs in vorticity-velocity formulation. Using a primitive variable formulation, Pereira et al. [42] provided a finite volume (FV) compact technique for discretizing the incompressible NSEs with fourth-order accuracy. Of late, the unstable incompressible NSEs in the velocity-pressure representation were published by Johnston and Liu [21], along with a numerical technique of order two applied to a non-staggered mesh, which is suitable for simulations with moderate to high Reynolds numbers. Kalita et al. [22] developed a group of compact schemes of higher order with weighted time steps efficiently capturing both transient and steady solutions for the 2D unsteady convection-diffusion equations with non-constant convection coefficients. NSEs have been investigated with the help of a finite difference formulation for compressible jet flow with small Reynolds number [12, 13]. Mohanty et al. [35, 36] developed two-level nine-point implicit finite difference methods in which arithmetic average discretization is performed to get the solution of the 2D non-linear PPDEs without necessitating the use of any fictitious points for the purpose of calculation when implemented to problems with a singular value. For the 2D steady-state incompressible Navier-Stokes equations, Bai et al. [4] constructed and analyzed the approximated incomplete LU factorization and the approximated unsymmetric Gauss-Seidel splitting preconditioning matrices for the coefficient matrix of the discretized linear system. Mittal et al. [32, 43] employed bi-cubic B-spline functions to find out numerical solutions of 2D unsteady advection diffusion equations. Aggul and Labovsky [2] combined the defect and deferred correction schemes to compute the solutions of NSE at high Reynolds number, which is second-order accurate in both space and time.

Talking about recent developments, the 2D unstable advection diffusion problem is solved by Mittal et al. [31] with the use of cubic B-spline quasi-interpolation approach through the Kronecker product. Employing the meshfree RBF-FD methodology, Abbaszadeh and Dehghan [1] developed an effective numerical method to simulate the time-dependent incompressible NSE with changing density. Recently, Saray et al. [39] used the multi-wavelet Galerkin method for the approximate solution of the 2D Burgers' equation. Alternating Direction Implicit (ADI) methods [14, 41] that reduce a multidimensional problem successively to independent one-dimensional problems, have proven to be efficient and are extensively utilised in a wide variety of contexts for numerically treating parabolic problems. In recent years, compact ADI techniques of higher accuracy for 2D parabolic equations have been discussed by numerous researchers (see Dai and Nassar [7], Karaa and Zhang [24] and references therein). Bashan [52] obtained efficient numerical solutions to coupled viscous Burgers' equations with very high Reynolds numbers via the contribution of the finite difference method and differential quadrature technique. The modified cubic B-spline differential quadrature method has been used to determine numerical solutions of the nonlinear modified Burgers' equation in [53]. Mohanty have proposed highly accurate approximations in exponential form for nonlinear elliptic PDEs in [38, 56].

Compact finite difference scheme is one which utilizes grid points located directly adjacent to the node about which the differences are taken. For three variables (x, y, t), compact finite difference scheme requires either 19- or 27-grid points on a cubical cell, whereas, in our work, we have formulated two-level compact finite difference method in exponential form for the second-order parabolic partial differential equations utilizing only nine nodes of a compact stencil at each time level. That means we are using only 18-grid points, and our method is fourth-order accurate in space and second-order accurate in time direction. Further, using the same (9+9)-grid points, we have written our method in vector form to solve system of nonlinear 2D parabolic equations. Further, we have constructed the ADI method for linear unsteady diffusion-convection equation which is shown to be unconditionally stable. In this case, we use a tri-diagonal solver to compute the method directly. Our numerical results show that the proposed exponential scheme solves a wide range of physical issues with great accuracy compared to the existing methods.

This investigation also considers the general 2D quasi-linear PPDE of order four, shown in the following form:

$$A\left(x, y, t\right)\ \nabla^4 u + u_t = \varphi\left(x, y, t, u, u_x, u_y, \nabla^2 u, \nabla^2 u_x, \nabla^2 u_y\right), \quad (x, y, t) \in \Omega_2, \tag{1.5}$$

with the initial condition:

$$u\left(x, y, 0\right) = \varphi_0\left(x, y\right), \quad 0 \le x, y \le a, \tag{1.6}$$

and the following boundary conditions:

$$\begin{aligned}
&u(x,0,t)=\varphi_1(x,t)\,,\;\; \frac{\partial^2 u}{\partial y^2}(x,0,t)=\varphi_2(x,t)\,,\;\; 0\le x\le a,\;\; t>0,\\
&u(x,a,t)=\varphi_3(x,t)\,,\;\; \frac{\partial^2 u}{\partial y^2}(x,a,t)=\varphi_4(x,t)\,,\;\; 0\le x\le a,\;\; t>0,\\
&u(0,y,t)=\psi_1(y,t)\,,\;\; \frac{\partial^2 u}{\partial x^2}(0,y,t)=\psi_2(y,t)\,,\;\; 0\le y\le a,\;\; t>0,\\
&u(a,y,t)=\psi_3(y,t)\,,\;\; \frac{\partial^2 u}{\partial x^2}(a,y,t)=\psi_4(y,t)\,,\;\; 0\le y\le a,\;\; t>0,
\end{aligned}\tag{1.7}$$

where $\nabla^2 u=\frac{\partial^2 u}{\partial x^2}+\frac{\partial^2 u}{\partial y^2}$ is the representation of the Laplacian operator of the function $u(x,y,t)$ in two space dimensions. Assume that the functions $\varphi_0,\varphi_i,\psi_i, i=1,\ldots,4$ are smooth enough, and their derivatives of all required orders may be found in the solution domain. Equations of this form formulate many applied mathematical models, like pattern generation in bistable systems [9], domain wall propagation in crystals formed by liquid [50], and travelling waves found in reaction-diffusion models [3]. These are few examples of situations where the Extended Fisher Kolmogorov (EFK) problem exists. In order to characterize the phase dynamics of reaction-diffusion models and the inherent instabilities of laminar flame fronts, the Kuramoto-Sivashinsky (KS) equation was developed [27, 44]. Because of its complexity and its capacity to express processes that occur in the real world, the KS equation has garnered huge attention over the course of the past few decades.

Fourth-order PPDEs have been the subject of a great deal of previous research on numerical approximation. Orthogonal cubic spline collocation of order two was utilized by Danumjaya and Pani [8] for the study of convergence of approximations to the EFK equation. The fourth-order diffusion equation in two dimensions is treated by Guo and Lü [17] using parallel difference schemes. The 2D EFK problem was solved using a three-stage linearly implicit finite difference approach, which is second-order convergent both in time and space variables [18]. Khiari and Omrani [26] proposed an application of a second-order Crank-Nicolson type finite difference scheme to the solution of the EFK equation in two spatial dimensions subject to Dirichlet boundary data. In [51], the approximate solutions of the fourth order extended Fisher-Kolmogorov equation have been obtained by applying the modified cubic B-spline based differential quadrature technique. In recent years, Liu et al. [29] presented a pseudo-spectral Fourier method to approximate the EFK equation in the two-dimensional space domain. A technique that relies on radial basis function and finite difference was developed by Dehghan and Shafieeabyaneh [11] to solve one, two, and three-dimensional cases of the EFK equation numerically. Ilati and Dehghan [20] suggested the solution of the EFK problem by using the local boundary integral equation technique. Omrani [40] examined a linearised finite difference discretization of the second order as a method for solving the non-linear evolutionary Sivashinsky equation. Kalogirou et al. [23] performed a thorough numerical examination of the 2D KS equation. Lately, Dehghan and Mohammadi [10] solved the damped KS problem in two dimensions using a numerical approach that is based on an explicit Runge-Kutta in exponential form in time and a meshless method in space. To study two-dimensional time-dependent parabolic PDEs, Mohammadi and Dehghan applied the boundary knot method (BKM) combined with the meshless analog equation method (MAEM) in space and a semi-implicit scheme in time [60]. Recently, Mohammadi and Dehghan [61] considered the radial basis function-generated finite difference scheme for space and an implicit-explicit time discretization is employed to deal with the time variable for the numerical solution of 2D parabolic PDEs. The introduction and increasing acceptance of compact methods rekindled interest in the discretization of biharmonic problems. In recent years, compact difference approaches for 2D quasi-linear parabolic problems of order four have been proposed [34, 37]. Mohanty and Sharma [57] presented a new compact 2-level implicit numerical method in the form of exponential approximation for finding the approximate solution of one-dimensional nonlinear fourth-order Kuramoto-Sivashinsky and Fisher-Kolmogorov equations. The described method has an accuracy of temporal order two and a spatial order three (or four) on a variable (or constant) mesh. Later on, they constructed a numerical scheme in exponential form based on off-step variable (or constant) mesh discretization for the numerical solution of a one-dimensional quasi-linear parabolic equation [58].

One of the main contributions of this study is that the proposed method is also applied to solve fourth-order parabolic partial differential equations without requiring any fictitious point to incorporate the boundary conditions and without any compromise with its accuracy. The proposed numerical scheme has been successfully applied to solve numerous benchmark problems such as the Navier-Stokes equation, the Taylor-Vortex equation, the Extended Fisher Kolmogorov equation, the Kuramoto-Sivashinsky equation, etc., and to verify the accuracy of the proposed method.

A general overview of the paper is provided here. In the next section, we introduce as well as construct two-level implicit difference method for the IBVPs (1.1)-(1.4). The proposed technique is generalized for system of quasi-linear PPDEs and applied to the fourth-order parabolic problem (1.5)-(1.7) in Section 3. Further, in Section 4, we explain the ADI scheme for a 2D linear parabolic equation and perform the Von-Neumann examination for the scheme's stability. Extensive numerical experiments of physical significance are described in Section 5 together with a comparative description to illustrate the accuracy and use of the suggested technique. Lastly, we give our concluding remarks in Section 6.

2 Two-level compact difference method: Formulation and derivation

Choosing $h > 0, k > 0$ and a positive integer N such that $h = \dfrac{a}{N+1}$, we describe a rectangular grid with the internal grid points $\left(x_\beta, y_\varrho, t_\sigma\right)$, $x_\beta = \beta h$, $y_\varrho = \varrho h$, $t_\sigma = \sigma k$, where $\beta, \varrho = 0, 1, \ldots, N+1$, and $\sigma = 0, 1, 2, \ldots$. Besides, let λ denote the mesh ratio $\dfrac{k}{h^2}$, $u^\sigma_{\beta,\varrho}$ and $U^\sigma_{\beta,\varrho}$ be the analytical and approximate solution of the function $u\,(x, y, t)$ at grid point $\left(x_\beta, y_\varrho, t_\sigma\right)$, respectively. Let $A^\sigma_{\beta,\varrho} = A\left(x_\beta, y_\varrho, t_\sigma\right)$, $C^\sigma_{\beta,\varrho} = C\left(x_\beta, y_\varrho, t_\sigma\right)$, etc. At the grid point $\left(x_\beta, y_\varrho, t_\sigma\right)$, the PPDE (1.1) can be described in the following way:

$$A^{\sigma}_{\beta,\varrho}U^{\sigma}_{xx_{\beta,\varrho}}+C^{\sigma}_{\beta,\varrho}U^{\sigma}_{yy_{\beta,\varrho}}=f\left(x_{\beta},y_{\varrho},t_{\sigma},U^{\sigma}_{\beta,\varrho},U^{\sigma}_{x_{\beta,\varrho}},U^{\sigma}_{y_{\beta,\varrho}},U^{\sigma}_{t_{\beta,\varrho}}\right)=F^{\sigma}_{\beta,\varrho} \tag{2.1}$$

For $m,n=0,\pm1$, the following approximations are defined for the solution value U and the co-efficients A,C at the grid point $\left(x_{\beta},y_{\varrho},\bar{t}_{\sigma}\right)$:

$$\bar{t}_{\sigma}=t_{\sigma}+\theta k,\ 0<\theta<1, \tag{2.2}$$

$$\overline{A}^{\sigma}_{\beta,\varrho}=A\left(x_{\beta},y_{\varrho},\bar{t}_{\sigma}\right), \tag{2.3}$$

$$\overline{A}^{\sigma}_{x_{\beta,\varrho}}=A_{x}\left(x_{\beta},y_{\varrho},\bar{t}_{\sigma}\right), \tag{2.4}$$

$$\overline{A}^{\sigma}_{y_{\beta,\varrho}}=A_{y}\left(x_{\beta},y_{\varrho},\bar{t}_{\sigma}\right), \tag{2.5}$$

$$\overline{A}^{\sigma}_{xx_{\beta,\varrho}}=A_{xx}\left(x_{\beta},y_{\varrho},\bar{t}_{\sigma}\right), \tag{2.6}$$

$$\overline{A}^{\sigma}_{yy_{\beta,\varrho}}=A_{yy}\left(x_{\beta},y_{\varrho},\bar{t}_{\sigma}\right), \tag{2.7}$$

$$\overline{C}^{\sigma}_{\beta,\varrho}=C\left(x_{\beta},y_{\varrho},\bar{t}_{\sigma}\right), \tag{2.8}$$

$$\overline{C}^{\sigma}_{x_{\beta,\varrho}}=C_{x}\left(x_{\beta},y_{\varrho},\bar{t}_{\sigma}\right), \tag{2.9}$$

$$\overline{C}^{\sigma}_{y_{\beta,\varrho}}=C_{y}\left(x_{\beta},y_{\varrho},\bar{t}_{\sigma}\right), \tag{2.10}$$

$$\overline{C}^{\sigma}_{xx_{\beta,\varrho}}=C_{xx}\left(x_{\beta},y_{\varrho},\bar{t}_{\sigma}\right), \tag{2.11}$$

$$\overline{C}^{\sigma}_{yy_{\beta,\varrho}}=C_{yy}\left(x_{\beta},y_{\varrho},\bar{t}_{\sigma}\right), \tag{2.12}$$

$$\overline{U}^{\sigma}_{\beta+m,\varrho+n}=\theta U^{\sigma+1}_{\beta+m,\varrho+n}+(1-\theta)U^{\sigma}_{\beta+m,\varrho+n}, \tag{2.13}$$

$$\overline{U}^{\sigma}_{x_{\beta,\varrho}}=\frac{\overline{U}^{\sigma}_{\beta+1,\varrho}-\overline{U}^{\sigma}_{\beta-1,\varrho}}{2h}, \tag{2.14}$$

$$\overline{U}^{\sigma}_{y_{\beta,\varrho}}=\frac{\overline{U}^{\sigma}_{\beta,\varrho+1}-\overline{U}^{\sigma}_{\beta,\varrho-1}}{2h}, \tag{2.15}$$

$$\overline{U}^{\sigma}_{t_{\beta,\varrho}}=\frac{U^{\sigma+1}_{\beta,\varrho}-U^{\sigma}_{\beta,\varrho}}{k}, \tag{2.16}$$

$$\overline{U}^{\sigma}_{t_{\beta\pm1,\varrho}}=\frac{U^{\sigma+1}_{\beta\pm1,\varrho}-U^{\sigma}_{\beta\pm1,\varrho}}{k}, \tag{2.17}$$

$$\overline{U}^{\sigma}_{t_{\beta,\varrho\pm1}}=\frac{U^{\sigma+1}_{\beta,\varrho\pm1}-U^{\sigma}_{\beta,\varrho\pm1}}{k}, \tag{2.18}$$

$$\overline{U}^{\sigma}_{x_{\beta\pm1,\varrho}}=\frac{\pm3\overline{U}^{\sigma}_{\beta\pm1,\varrho}\mp4\overline{U}^{\sigma}_{\beta,\varrho}\pm\overline{U}^{\sigma}_{\beta\mp1,\varrho}}{2h}, \tag{2.19}$$

$$\overline{U}^{\sigma}_{x_{\beta,\varrho\pm1}} = \frac{\overline{U}^{\sigma}_{\beta+1,\varrho\pm1} - \overline{U}^{\sigma}_{\beta-1,\varrho\pm1}}{2h}, \tag{2.20}$$

$$\overline{U}^{\sigma}_{y_{\beta\pm1,\varrho}} = \frac{\overline{U}^{\sigma}_{\beta\pm1,\varrho+1} - \overline{U}^{\sigma}_{\beta\pm1,\varrho-1}}{2h}, \tag{2.21}$$

$$\overline{U}^{\sigma}_{y_{\beta,\varrho\pm1}} = \frac{\pm3\overline{U}^{\sigma}_{\beta,\varrho\pm1} \mp 4\overline{U}^{\sigma}_{\beta,\varrho} \pm \overline{U}^{\sigma}_{\beta,\varrho\mp1}}{2h}, \tag{2.22}$$

$$\overline{U}^{\sigma}_{xx_{\beta,\varrho}} = \frac{\overline{U}^{\sigma}_{\beta+1,\varrho} - 2\overline{U}^{\sigma}_{\beta,\varrho} + \overline{U}^{\sigma}_{\beta-1,\varrho}}{h^2}, \tag{2.23}$$

$$\overline{U}^{\sigma}_{yy_{\beta,\varrho}} = \frac{\overline{U}^{\sigma}_{\beta,\varrho+1} - 2\overline{U}^{\sigma}_{\beta,\varrho} + \overline{U}^{\sigma}_{\beta,\varrho-1}}{h^2}, \tag{2.24}$$

$$\overline{U}^{\sigma}_{xxy_{\beta,\varrho}} = \frac{\overline{U}^{\sigma}_{xx_{\beta,\varrho+1}} - \overline{U}^{\sigma}_{xx_{\beta,\varrho-1}}}{2h}, \tag{2.25}$$

$$\overline{U}^{\sigma}_{xyy_{\beta,\varrho}} = \frac{\overline{U}^{\sigma}_{yy_{\beta+1,\varrho}} - \overline{U}^{\sigma}_{yy_{\beta-1,\varrho}}}{2h}, \tag{2.26}$$

$$\overline{U}^{\sigma}_{xxyy_{\beta,\varrho}} = \frac{\overline{U}^{\sigma}_{xx_{\beta,\varrho+1}} - 2\overline{U}^{\sigma}_{xx_{\beta,\varrho}} + \overline{U}^{\sigma}_{xx_{\beta,\varrho-1}}}{h^2}. \tag{2.27}$$

Furthermore, we define the following approximations:

$$\overline{F}^{\sigma}_{\beta\pm1,\varrho} = f\left(x_{\beta\pm1}, y_{\varrho}, \bar{t}_{\sigma}, \overline{U}^{\sigma}_{\beta\pm1,\varrho}, \overline{U}^{\sigma}_{x_{\beta\pm1,\varrho}}, \overline{U}^{\sigma}_{y_{\beta\pm1,\varrho}}, \overline{U}^{\sigma}_{t_{\beta\pm1,\varrho}}\right), \tag{2.28}$$

$$\overline{F}^{\sigma}_{\beta,\varrho\pm1} = f\left(x_{\beta}, y_{\varrho\pm1}, \bar{t}_{\sigma}, \overline{U}^{\sigma}_{\beta,\varrho\pm1}, \overline{U}^{\sigma}_{x_{\beta,\varrho\pm1}}, \overline{U}^{\sigma}_{y_{\beta,\varrho\pm1}}, \overline{U}^{\sigma}_{t_{\beta,\varrho\pm1}}\right), \tag{2.29}$$

$$\overline{\overline{U}}^{\sigma}_{x_{\beta,\varrho}} = \overline{U}^{\sigma}_{x_{\beta,\varrho}} + a_1 h\left(\overline{F}^{\sigma}_{\beta+1,\varrho} - \overline{F}^{\sigma}_{\beta-1,\varrho}\right) + 2a_2h^2\overline{U}^{\sigma}_{xyy_{\beta,\varrho}} + 2h^2\left(a_3\overline{U}^{\sigma}_{xx_{\beta,\varrho}} + a_4\overline{U}^{\sigma}_{yy_{\beta,\varrho}}\right), \tag{2.30}$$

$$\overline{\overline{U}}^{\sigma}_{y_{\beta,\varrho}} = \overline{U}^{\sigma}_{y_{\beta,\varrho}} + b_1 h\left(\overline{F}^{\sigma}_{\beta,\varrho+1} - \overline{F}^{\sigma}_{\beta,\varrho-1}\right) + 2b_2h^2\overline{U}^{\sigma}_{xxy_{\beta,\varrho}} + 2h^2\left(b_3\overline{U}^{\sigma}_{xx_{\beta,\varrho}} + b_4\overline{U}^{\sigma}_{yy_{\beta,\varrho}}\right), \tag{2.31}$$

$$\overline{\overline{F}}^{\sigma}_{\beta,\varrho} = f\left(x_{\beta}, y_{\varrho}, \bar{t}_{\sigma}, \overline{U}^{\sigma}_{\beta,\varrho}, \overline{\overline{U}}^{\sigma}_{x_{\beta,\varrho}}, \overline{\overline{U}}^{\sigma}_{y_{\beta,\varrho}}, \overline{U}^{\sigma}_{t_{\beta,\varrho}}\right), \tag{2.32}$$

$$\widehat{\widehat{U}}^{\sigma}_{x_{\beta,\varrho}} = \overline{U}^{\sigma}_{x_{\beta,\varrho}} + c_1 h\left(\overline{F}^{\sigma}_{\beta+1,\varrho} - \overline{F}^{\sigma}_{\beta-1,\varrho}\right) + 2c_2h^2\overline{U}^{\sigma}_{xyy_{\beta,\varrho}} + 2h^2\left(c_3\overline{U}^{\sigma}_{xx_{\beta,\varrho}} + c_4\overline{U}^{\sigma}_{yy_{\beta,\varrho}}\right), \tag{2.33}$$

$$\widehat{\widehat{U}}^{\sigma}_{y_{\beta,\varrho}} = \overline{U}^{\sigma}_{y_{\beta,\varrho}} + d_1 h\left(\overline{F}^{\sigma}_{\beta,\varrho+1} - \overline{F}^{\sigma}_{\beta,\varrho-1}\right) + 2d_2h^2\overline{U}^{\sigma}_{xxy_{\beta,\varrho}} + 2h^2\left(d_3\overline{U}^{\sigma}_{xx_{\beta,\varrho}} + d_4\overline{U}^{\sigma}_{yy_{\beta,\varrho}}\right), \tag{2.34}$$

$$\widehat{\widehat{F}}^{\sigma}_{\beta,\varrho} = f\left(x_{\beta}, y_{\varrho}, \bar{t}_{\sigma}, \overline{U}^{\sigma}_{\beta,\varrho}, \widehat{\widehat{U}}^{\sigma}_{x_{\beta,\varrho}}, \widehat{\widehat{U}}^{\sigma}_{y_{\beta,\varrho}}, \overline{U}^{\sigma}_{t_{\beta,\varrho}}\right), \tag{2.35}$$

where a_i, b_i, c_i and d_i, $i = 1, \ldots, 4$, are unknowns to be determined.

Now, utilizing fourth-order compact technique from [38], Taylor's series expansion, and some algebraic calculations, we write equation (2.1) as follows:

$$L\left[U\right]=\left[L_1U^{\sigma}_{xx_{\beta,\varrho}}+L_2U^{\sigma}_{yy_{\beta,\varrho}}+L_3U^{\sigma}_{xxy_{\beta,\varrho}}+L_4U^{\sigma}_{xyy_{\beta,\varrho}}+L_5U^{\sigma}_{xxyy_{\beta,\varrho}}\right]$$
$$=F^{\sigma}_{\beta,\varrho}\exp\left(\frac{J_1F^{\sigma}_{\beta+1,\varrho}+J_2F^{\sigma}_{\beta-1,\varrho}+J_3F^{\sigma}_{\beta,\varrho+1}+J_4F^{\sigma}_{\beta,\varrho-1}-4F^{\sigma}_{\beta,\varrho}}{12F^{\sigma}_{\beta,\varrho}}\right)+O(h^4), \tag{2.36}$$

where

$$L_1=A^{\sigma}_{\beta,\varrho}+\frac{h^2}{12}\left(A^{\sigma}_{xx_{\beta,\varrho}}+A^{\sigma}_{yy_{\beta,\varrho}}\right)-\left(\frac{hA^{\sigma}_{x_{\beta,\varrho}}}{6A^{\sigma}_{\beta,\varrho}}\right)hA^{\sigma}_{x_{\beta,\varrho}}-\left(\frac{hC^{\sigma}_{y_{\beta,\varrho}}}{6C^{\sigma}_{\beta,\varrho}}\right)hA^{\sigma}_{y_{\beta,\varrho}},$$
$$L_2=C^{\sigma}_{\beta,\varrho}+\frac{h^2}{12}\left(C^{\sigma}_{xx_{\beta,\varrho}}+C^{\sigma}_{yy_{\beta,\varrho}}\right)-\left(\frac{hA^{\sigma}_{x_{\beta,\varrho}}}{6A^{\sigma}_{\beta,\varrho}}\right)hC^{\sigma}_{x_{\beta,\varrho}}-\left(\frac{hC^{\sigma}_{y_{\beta,\varrho}}}{6C^{\sigma}_{\beta,\varrho}}\right)hC^{\sigma}_{y_{\beta,\varrho}},$$

$L_3=\dfrac{h^2}{6}\left[A^{\sigma}_{y_{\beta,\varrho}}-\dfrac{C^{\sigma}_{y_{\beta,\varrho}}}{C^{\sigma}_{\beta,\varrho}}A^{\sigma}_{\beta,\varrho}\right]$, $L_4=\dfrac{h^2}{6}\left[C^{\sigma}_{x_{\beta,\varrho}}-\dfrac{A^{\sigma}_{x_{\beta,\varrho}}}{A^{\sigma}_{\beta,\varrho}}C^{\sigma}_{\beta,\varrho}\right]$, $L_5=h^2\left[\dfrac{A^{\sigma}_{\beta,\varrho}+C^{\sigma}_{\beta,\varrho}}{12}\right]$, and

$J_1=1-h\dfrac{A^{\sigma}_{x_{\beta,\varrho}}}{A^{\sigma}_{\beta,\varrho}}$, $J_2=1+h\dfrac{A^{\sigma}_{x_{\beta,\varrho}}}{A^{\sigma}_{\beta,\varrho}}$, $J_3=1-h\dfrac{C^{\sigma}_{y_{\beta,\varrho}}}{C^{\sigma}_{\beta,\varrho}}$, $J_4=1+h\dfrac{C^{\sigma}_{y_{\beta,\varrho}}}{C^{\sigma}_{\beta,\varrho}}$.

At the grid points $\left(x_\beta, y_\varrho, t_\sigma\right)$, we denote

$$\omega=\left(\frac{\partial F}{\partial t}\right)^{\sigma}_{\beta,\varrho},\ \zeta=\left(\frac{\partial F}{\partial U}\right)^{\sigma}_{\beta,\varrho},\ \gamma=\left(\frac{\partial F}{\partial U_x}\right)^{\sigma}_{\beta,\varrho},$$
$$\xi=\left(\frac{\partial F}{\partial U_y}\right)^{\sigma}_{\beta,\varrho},\ \eta=\left(\frac{\partial F}{\partial U_t}\right)^{\sigma}_{\beta,\varrho}. \tag{2.37}$$

Differentiating equation (1.1) with respect to t at the grid points $\left(x_\beta, y_\varrho, t_\sigma\right)$ and using (2.37), we get

$$A^{\sigma}_{\beta,\varrho}U^{\sigma}_{xxt_{\beta,\varrho}}+A^{\sigma}_{t_{\beta,\varrho}}U^{\sigma}_{xx_{\beta,\varrho}}+C^{\sigma}_{\beta,\varrho}U^{\sigma}_{yyt_{\beta,\varrho}}+C^{\sigma}_{t_{\beta,\varrho}}U^{\sigma}_{yy_{\beta,\varrho}}$$
$$=\omega+\zeta U^{\sigma}_{t_{\beta,\varrho}}+\gamma U^{\sigma}_{xt_{\beta,\varrho}}+\xi U^{\sigma}_{yt_{\beta,\varrho}}+\eta U^{\sigma}_{tt_{\beta,\varrho}} \tag{2.38}$$

Then, using approximations (2.2), (2.13), (2.17)-(2.22) and (2.37), we simplify (2.28)-(2.29), yielding

$$\overline{F}^{\sigma}_{\beta\pm1,\varrho}=F^{\sigma}_{\beta\pm1,\varrho}+\frac{k}{2}T_1+\frac{h^2}{6}T_2+O\left(k^2\pm kh\pm h^3+kh^2+h^4\right), \tag{2.39}$$

$$\overline{F}^{\sigma}_{\beta,\varrho\pm1}=F^{\sigma}_{\beta,\varrho\pm1}+\frac{k}{2}T_1+\frac{h^2}{6}T_3+O\left(k^2\pm kh\pm h^3+kh^2+h^4\right), \tag{2.40}$$

where

$$T_1 = 2\theta\left(\omega + \zeta\, U^{\sigma}_{t_{\beta,\varrho}} + \gamma U^{\sigma}_{xt_{\beta,\varrho}} + \xi U^{\sigma}_{yt_{\beta,\varrho}}\right) + \eta U^{\sigma}_{tt_{\beta,\varrho}},$$

$$T_2 = -2\gamma U^{\sigma}_{xxx_{\beta,\varrho}} + \xi U^{\sigma}_{yyy_{\beta,\varrho}}, \quad T_3 = \gamma U^{\sigma}_{xxx_{\beta,\varrho}} - 2\xi U^{\sigma}_{yyy_{\beta,\varrho}}.$$

Again, taking into account the equations (2.14)-(2.15), (2.23)-(2.24), (2.25)-(2.26), (2.30)-(2.31) and (2.39)-(2.40), we get

$$\overline{\overline{U}}^{\sigma}_{x_{\beta,\varrho}} = U^{\sigma}_{x_{\beta,\varrho}} + \theta k U^{\sigma}_{xt_{\beta,\varrho}} + \frac{h^2}{6}\Big[\left(1+12a_1 A^{\sigma}_{\beta,\varrho}\right)U^{\sigma}_{xxx_{\beta,\varrho}} + 12\left(a_1 C^{\sigma}_{\beta,\varrho} + a_2\right)U^{\sigma}_{xyy_{\beta,\varrho}}$$
$$+ 12\left(a_1 A^{\sigma}_{x_{\beta,\varrho}} + a_3\right)U^{\sigma}_{xx_{\beta,\varrho}} + 12\left(a_1 C^{\sigma}_{x_{\beta,\varrho}} + a_4\right)U^{\sigma}_{yy_{\beta,\varrho}}\Big] + O\left(k^2 + kh^2 + h^4\right),$$

$$\overline{\overline{U}}^{\sigma}_{y_{\beta,\varrho}} = U^{\sigma}_{y_{\beta,\varrho}} + \theta k U^{\sigma}_{yt_{\beta,\varrho}} + \frac{h^2}{6}\Big[\left(1+12b_1 C^{\sigma}_{\beta,\varrho}\right)U^{\sigma}_{yyy_{\beta,\varrho}} + 12\left(b_1 A^{\sigma}_{\beta,\varrho} + b_2\right)U^{\sigma}_{xxy_{\beta,\varrho}}$$
$$+ 12\left(b_1 A^{\sigma}_{y_{\beta,\varrho}} + b_3\right)U^{\sigma}_{xx_{\beta,\varrho}} + 12\left(b_1 C^{\sigma}_{y_{\beta,\varrho}} + b_4\right)U^{\sigma}_{yy_{\beta,\varrho}}\Big] + O\left(k^2 + kh^2 + h^4\right),$$

which get reduced to

$$\overline{\overline{U}}^{\sigma}_{x_{\beta,\varrho}} = U^{\sigma}_{x_{\beta,\varrho}} + \theta k U^{\sigma}_{xt_{\beta,\varrho}} + O\left(k^2 + kh^2 + h^4\right), \tag{2.41}$$

$$\overline{\overline{U}}^{\sigma}_{y_{\beta,\varrho}} = U^{\sigma}_{y_{\beta,\varrho}} + \theta k U^{\sigma}_{yt_{\beta,\varrho}} + O\left(k^2 + kh^2 + h^4\right), \tag{2.42}$$

for the following value of parameters

$$a_1 = \frac{-1}{12A^{\sigma}_{\beta,\varrho}}, \quad a_2 = \frac{C^{\sigma}_{\beta,\varrho}}{12A^{\sigma}_{\beta,\varrho}}, \quad a_3 = \frac{A^{\sigma}_{x_{\beta,\varrho}}}{12A^{\sigma}_{\beta,\varrho}}, \quad a_4 = \frac{C^{\sigma}_{x_{\beta,\varrho}}}{12A^{\sigma}_{\beta,\varrho}},$$

$$b_1 = \frac{-1}{12C^{\sigma}_{\beta,\varrho}}, \quad b_2 = \frac{A^{\sigma}_{\beta,\varrho}}{12C^{\sigma}_{\beta,\varrho}}, \quad b_3 = \frac{A^{\sigma}_{y_{\beta,\varrho}}}{12C^{\sigma}_{\beta,\varrho}}, \quad b_4 = \frac{C^{\sigma}_{y_{\beta,\varrho}}}{12C^{\sigma}_{\beta,\varrho}}.$$

Now, with the aid of the equations (2.2), (2.13), (2.16), (2.37), (2.41)-(2.42), approximation (2.32) can be represented as:

$$\overline{\overline{F}}^{\sigma}_{\beta,\varrho} = F^{\sigma}_{\beta,\varrho} + \frac{k}{2}T_1 + O\left(k^2 + kh^2 + h^4\right) \tag{2.43}$$

Next, we rewrite (2.33) and (2.34) with the help of approximations (2.14)-(2.15), (2.23)-(2.24), (2.25)-(2.26) and (2.39)-(2.40) as:

$$\widehat{\widehat{U}}^{\sigma}_{x_{\beta,\varrho}} = U^{\sigma}_{x_{\beta,\varrho}} + \theta k U^{\sigma}_{xt_{\beta,\varrho}} + \frac{h^2}{6}T_4 + O\left(k^2 + kh^2 + h^4\right), \tag{2.44}$$

$$\widehat{\widehat{U}}^{\sigma}_{y_{\beta,\varrho}} = U^{\sigma}_{y_{\beta,\varrho}} + \theta k U^{\sigma}_{yt_{\beta,\varrho}} + \frac{h^2}{6} T_5 + O\left(k^2 + kh^2 + h^4\right), \tag{2.45}$$

where

$$T_4 = \left(1 + 12 c_1 A^{\sigma}_{\beta,\varrho}\right) U^{\sigma}_{xxx_{\beta,\varrho}} + 12\left(c_1 C^{\sigma}_{\beta,\varrho} + c_2\right) U^{\sigma}_{xyy_{\beta,\varrho}} + 12\left(c_1 A^{\sigma}_{x_{\beta,\varrho}} + c_3\right) U^{\sigma}_{xx_{\beta,\varrho}} + 12\left(c_1 C^{\sigma}_{x_{\beta,\varrho}} + c_4\right) U^{\sigma}_{yy_{\beta,\varrho}},$$

$$T_5 = \left(1 + 12 d_1 C^{\sigma}_{\beta,\varrho}\right) U^{\sigma}_{yyy_{\beta,\varrho}} + 12\left(d_1 A^{\sigma}_{\beta,\varrho} + d_2\right) U^{\sigma}_{xxy_{\beta,\varrho}} + 12\left(d_1 A^{\sigma}_{y_{\beta,\varrho}} + d_3\right) U^{\sigma}_{xx_{\beta,\varrho}} + 12\left(d_1 C^{\sigma}_{y_{\beta,\varrho}} + d_4\right) U^{\sigma}_{yy_{\beta,\varrho}}.$$

Using (2.2), (2.13), (2.16), (2.37), (2.44) and (2.45), the approximation (2.35) can be expressed as:

$$\widehat{\widehat{F}}^{\sigma}_{\beta,\varrho} = F^{\sigma}_{\beta,\varrho} + \frac{k}{2} T_1 + \frac{h^2}{6}\gamma T_4 + \frac{h^2}{6}\xi T_5 + O\left(k^2 + kh^2 + h^4\right) \tag{2.46}$$

On simplifying (2.3)-(2.12), we get

$$\overline{A}^{\sigma}_{\beta,\varrho} = A^{\sigma}_{\beta,\varrho} + \theta k A^{\sigma}_{t_{\beta,\varrho}} + O\left(k^2\right), \tag{2.47}$$

$$\overline{A}^{\sigma}_{x_{\beta,\varrho}} = A^{\sigma}_{x_{\beta,\varrho}} + \theta k A^{\sigma}_{xt_{\beta,\varrho}} + O\left(k^2\right), \tag{2.48}$$

$$\overline{A}^{\sigma}_{y_{\beta,\varrho}} = A^{\sigma}_{y_{\beta,\varrho}} + \theta k A^{\sigma}_{yt_{\beta,\varrho}} + O\left(k^2\right), \tag{2.49}$$

$$\overline{A}^{\sigma}_{xx_{\beta,\varrho}} = A^{\sigma}_{xx_{\beta,\varrho}} + \theta k A^{\sigma}_{xxt_{\beta,\varrho}} + O\left(k^2\right), \tag{2.50}$$

$$\overline{A}^{\sigma}_{yy_{\beta,\varrho}} = A^{\sigma}_{yy_{\beta,\varrho}} + \theta k A^{\sigma}_{yyt_{\beta,\varrho}} + O\left(k^2\right), \tag{2.51}$$

$$\overline{C}^{\sigma}_{\beta,\varrho} = C^{\sigma}_{\beta,\varrho} + \theta k C^{\sigma}_{t_{\beta,\varrho}} + O\left(k^2\right), \tag{2.52}$$

$$\overline{C}^{\sigma}_{x_{\beta,\varrho}} = C^{\sigma}_{x_{\beta,\varrho}} + \theta k C^{\sigma}_{xt_{\beta,\varrho}} + O\left(k^2\right), \tag{2.53}$$

$$\overline{C}^{\sigma}_{y_{\beta,\varrho}} = C^{\sigma}_{y_{\beta,\varrho}} + \theta k C^{\sigma}_{yt_{\beta,\varrho}} + O\left(k^2\right), \tag{2.54}$$

$$\overline{C}^{\sigma}_{xx_{\beta,\varrho}} = C^{\sigma}_{xx_{\beta,\varrho}} + \theta k C^{\sigma}_{xxt_{\beta,\varrho}} + O\left(k^2\right), \tag{2.55}$$

$$\overline{C}^{\sigma}_{yy_{\beta,\varrho}} = C^{\sigma}_{yy_{\beta,\varrho}} + \theta k C^{\sigma}_{yyt_{\beta,\varrho}} + O\left(k^2\right). \tag{2.56}$$

Then, in exponential form, a new technique is given by:

$$
\begin{aligned}
&L\left[\overline{U}\right]=\left[\overline{L}_1\overline{U}^{\sigma}_{xx_{\beta,\varrho}}+\overline{L}_2\overline{U}^{\sigma}_{yy_{\beta,\varrho}}+\overline{L}_3\overline{U}^{\sigma}_{xxy_{\beta,\varrho}}+\overline{L}_4\overline{U}^{\sigma}_{xyy_{\beta,\varrho}}+\overline{L}_5\overline{U}^{\sigma}_{xxyy_{\beta,\varrho}}\right]\\
&=\overline{\overline{F}}^{\sigma}_{\beta,\varrho}\exp\left(\frac{\overline{J}_1\overline{F}^{\sigma}_{\beta+1,\varrho}+\overline{J}_2\overline{F}^{\sigma}_{\beta-1,\varrho}+\overline{J}_3\overline{F}^{\sigma}_{\beta,\varrho+1}+\overline{J}_4\overline{F}^{\sigma}_{\beta,\varrho-1}-4\widehat{\overline{\overline{F}}}^{\sigma}_{\beta,\varrho}}{12\overline{\overline{F}}^{\sigma}_{\beta,\varrho}}\right)+\overline{T}^{\sigma}_{\beta,\varrho},
\end{aligned}
\tag{2.57}
$$

where $\overline{T}^{\sigma}_{\beta,\varrho}=O\left(k^2+kh^2+h^4\right)$ is the local truncation error (LTE) and the coefficients are given by:

$\overline{L}_1=\overline{A}^{\sigma}_{\beta,\varrho}+\dfrac{h^2}{12}\left(\overline{A}^{\sigma}_{xx_{\beta,\varrho}}+\overline{A}^{\sigma}_{yy_{\beta,\varrho}}\right)-\left(\dfrac{h\overline{A}^{\sigma}_{x_{\beta,\varrho}}}{6\overline{A}^{\sigma}_{\beta,\varrho}}\right)h\overline{A}^{\sigma}_{x_{\beta,\varrho}}-\left(\dfrac{h\overline{C}^{\sigma}_{y_{\beta,\varrho}}}{6\overline{C}^{\sigma}_{\beta,\varrho}}\right)h\overline{A}^{\sigma}_{y_{\beta,\varrho}},$

$\overline{L}_2=\overline{C}^{\sigma}_{\beta,\varrho}+\dfrac{h^2}{12}\left(\overline{C}^{\sigma}_{xx_{\beta,\varrho}}+\overline{C}^{\sigma}_{yy_{\beta,\varrho}}\right)-\left(\dfrac{h\overline{A}^{\sigma}_{x_{\beta,\varrho}}}{6\overline{A}^{\sigma}_{\beta,\varrho}}\right)h\overline{C}^{\sigma}_{x_{\beta,\varrho}}-\left(\dfrac{h\overline{C}^{\sigma}_{y_{\beta,\varrho}}}{6\overline{C}^{\sigma}_{\beta,\varrho}}\right)h\overline{C}^{\sigma}_{y_{\beta,\varrho}},$

$\overline{L}_3=\dfrac{h^2}{6}\left[\overline{A}^{\sigma}_{y_{\beta,\varrho}}-\dfrac{\overline{C}^{\sigma}_{y_{\beta,\varrho}}}{\overline{C}^{\sigma}_{\beta,\varrho}}\overline{A}^{\sigma}_{\beta,\varrho}\right]$, $\quad\overline{L}_4=\dfrac{h^2}{6}\left[\overline{C}^{\sigma}_{x_{\beta,\varrho}}-\dfrac{\overline{A}^{\sigma}_{x_{\beta,\varrho}}}{\overline{A}^{\sigma}_{\beta,\varrho}}\overline{C}^{\sigma}_{\beta,\varrho}\right]$, $\quad\overline{L}_5=h^2\left[\dfrac{\overline{A}^{\sigma}_{\beta,\varrho}+\overline{C}^{\sigma}_{\beta,\varrho}}{12}\right]$, and

$\overline{J}_1=1-h\dfrac{\overline{A}^{\sigma}_{x_{\beta,\varrho}}}{\overline{A}^{\sigma}_{\beta,\varrho}}$, $\overline{J}_2=1+h\dfrac{\overline{A}^{\sigma}_{x_{\beta,\varrho}}}{\overline{A}^{\sigma}_{\beta,\varrho}}$, $\overline{J}_3=1-h\dfrac{\overline{C}^{\sigma}_{y_{\beta,\varrho}}}{\overline{C}^{\sigma}_{\beta,\varrho}}$, $\overline{J}_4=1+h\dfrac{\overline{C}^{\sigma}_{y_{\beta,\varrho}}}{\overline{C}^{\sigma}_{\beta,\varrho}}$.

With the aid of (2.36), (2.38)-(2.40), (2.43) and (2.46)-(2.56), from (2.57), we obtain the LTE as:

$$
\begin{aligned}
\overline{T}^{\sigma}_{\beta,\varrho}&=k\left(\theta-\frac{1}{2}\right)\eta U^{\sigma}_{tt_{\beta,\varrho}}+\frac{h^2}{18}\left[\left(\frac{3}{2}+12c_1A^{\sigma}_{\beta,\varrho}\right)U^{\sigma}_{xxx_{\beta,\varrho}}+12\left(c_1C^{\sigma}_{\beta,\varrho}+c_2\right)U^{\sigma}_{xyy_{\beta,\varrho}}\right.\\
&\left.+12\left(c_1A^{\sigma}_{x_{\beta,\varrho}}+c_3\right)U^{\sigma}_{xx_{\beta,\varrho}}+12\left(c_1C^{\sigma}_{x_{\beta,\varrho}}+c_4\right)U^{\sigma}_{yy_{\beta,\varrho}}\right]\gamma+\frac{h^2}{18}\left[\left(\frac{3}{2}+12d_1C^{\sigma}_{\beta,\varrho}\right)U^{\sigma}_{yyy_{\beta,\varrho}}\right.\\
&\left.+12\left(d_1A^{\sigma}_{\beta,\varrho}+d_2\right)U^{\sigma}_{xxy_{\beta,\varrho}}+12\left(d_1A^{\sigma}_{y_{\beta,\varrho}}+d_3\right)U^{\sigma}_{xx_{\beta,\varrho}}+12\left(d_1C^{\sigma}_{y_{\beta,\varrho}}+d_4\right)U^{\sigma}_{yy_{\beta,\varrho}}\right]\xi\\
&+O\left(k^2+kh^2+h^4\right).
\end{aligned}
\tag{2.58}
$$

For the proposed method (2.57) to be of $O\left(k^2+kh^2+h^4\right)$, the coefficients of k, h^2 in (2.58) must be vanish. Thus, the values of parameters are given by:

$$\theta=\frac{1}{2},$$

$$c_1=\frac{-1}{8A^{\sigma}_{\beta,\varrho}},\quad c_2=\frac{C^{\sigma}_{\beta,\varrho}}{8A^{\sigma}_{\beta,\varrho}},\quad c_3=\frac{A^{\sigma}_{x_{\beta,\varrho}}}{8A^{\sigma}_{\beta,\varrho}},\quad c_4=\frac{C^{\sigma}_{x_{\beta,\varrho}}}{8A^{\sigma}_{\beta,\varrho}},$$

$$d_1=\frac{-1}{8C^{\sigma}_{\beta,\varrho}},\quad d_2=\frac{A^{\sigma}_{\beta,\varrho}}{8C^{\sigma}_{\beta,\varrho}},\quad d_3=\frac{A^{\sigma}_{y\beta,\varrho}}{8C^{\sigma}_{\beta,\varrho}},\quad d_4=\frac{C^{\sigma}_{y\beta,\varrho}}{8C^{\sigma}_{\beta,\varrho}},$$

and the local truncation error is $\overline{T}^{\sigma}_{\beta,\varrho}=O\left(k^2+kh^2+h^4\right)$.

Note that, $A>0, C>0$ in Ω_2. Thus, $L[U]$ is well defined. As $h\to 0, k\to 0$, it is easy to verify that

$\overline{A}^{\sigma}_{\beta,\varrho}\to A^{\sigma}_{\beta,\varrho}, \overline{A}^{\sigma}_{x\beta,\varrho}\to A^{\sigma}_{x\beta,\varrho}, \overline{A}^{\sigma}_{y\beta,\varrho}\to A^{\sigma}_{y\beta,\varrho}, \overline{A}^{\sigma}_{xx\beta,\varrho}\to A^{\sigma}_{xx\beta,\varrho}, \overline{A}^{\sigma}_{yy\beta,\varrho}\to A^{\sigma}_{yy\beta,\varrho}$,
$\overline{C}^{\sigma}_{\beta,\varrho}\to C^{\sigma}_{\beta,\varrho}, \overline{C}^{\sigma}_{x\beta,\varrho}\to C^{\sigma}_{x\beta,\varrho}, \overline{C}^{\sigma}_{y\beta,\varrho}\to C^{\sigma}_{y\beta,\varrho}, \overline{C}^{\sigma}_{xx\beta,\varrho}\to C^{\sigma}_{xx\beta,\varrho}, \overline{C}^{\sigma}_{yy\beta,\varrho}\to C^{\sigma}_{yy\beta,\varrho}$,
$\overline{L_1}\to L_1, \overline{L_2}\to L_2, \overline{L_3}\to L_3, \overline{L_4}\to L_4, \overline{L_5}\to L_5, \overline{J_1}\to J_1, \overline{J_2}\to J_2, \overline{J_3}\to J_3, \overline{J_4}\to J_4$,
$L[\overline{U}]\to L[U], \overline{F}^{\sigma}_{\beta\pm1,\varrho}\to F^{\sigma}_{\beta\pm1,\varrho}, \overline{F}^{\sigma}_{\beta,\varrho\pm1}\to F^{\sigma}_{\beta,\varrho\pm1}, \overline{\overline{F}}^{\sigma}_{\beta,\varrho}\to F^{\sigma}_{\beta,\varrho}, \widehat{\overline{F}}^{\sigma}_{\beta,\varrho}\to F^{\sigma}_{\beta,\varrho}$.

Thus, by the help of (2.36) and (2.57), it is easy to check that $\overline{T}^{\sigma}_{\beta,\varrho}\to 0$ as $h\to 0, k\to 0$. Hence, the approximation (2.57) is consistent with the PPDE (1.1). Since the solution of PPDE (1.1) exists and unique, and the approximation (2.57) is consistent with (1.1), hence the approximate solution exists and unique in the solution domain Ω_2.

3 Generalisation to the system of equations and application to fourth order PDEs

In this part of the article, we investigate the following quasi-linear PPDEs in vector form:

$$\begin{aligned}&\boldsymbol{A}(x,y,t)\frac{\partial^2\boldsymbol{u}}{\partial x^2}+\boldsymbol{C}(x,y,t)\frac{\partial^2\boldsymbol{u}}{\partial y^2}\\&=\boldsymbol{f}\left(x,y,t,u^{(1)},u^{(2)},\ldots,u^{(M)},u_x^{(1)},u_x^{(2)},\ldots,u_x^{(M)},u_y^{(1)},u_y^{(2)},\ldots,u_y^{(M)},u_t^{(1)},u_t^{(2)},\ldots,u_t^{(M)}\right),\end{aligned}\tag{3.1}$$

for $(x,y,t)\in\Omega_2$, subject to the following conditions in vector form:

$$\boldsymbol{u}(0,y,t)=\boldsymbol{f_0}(y,t),\ \boldsymbol{u}(a,y,t)=\boldsymbol{f_1}(y,t),\ 0<=y<=a, t>0,\tag{3.2}$$
$$\boldsymbol{u}(x,0,t)=\boldsymbol{g_0}(x,t),\ \boldsymbol{u}(x,a,t)=\boldsymbol{g_1}(x,t),\ 0<=x<=a, t>0,\tag{3.3}$$
$$\boldsymbol{u}(x,y,0)=\boldsymbol{u_0}(x,y),\ 0\le x,y\le a,\tag{3.4}$$

Here, $\boldsymbol{A}=\begin{bmatrix}A^{(1)}&&&\\&A^{(2)}&&\\&&\ddots&\\&&&A^{(M)}\end{bmatrix}$, $\boldsymbol{C}=\begin{bmatrix}C^{(1)}&&&\\&C^{(2)}&&\\&&\ddots&\\&&&C^{(M)}\end{bmatrix}$ are $M\times M$ diagonal matrices, and $\boldsymbol{u} = \begin{bmatrix} u^{(1)} \\ u^{(2)} \\ \vdots \\ u^{(M)} \end{bmatrix}$, $\boldsymbol{f} = \begin{bmatrix} f^{(1)} \\ f^{(2)} \\ \vdots \\ f^{(M)} \end{bmatrix}$ are vectors having M components each. And $\boldsymbol{u_0}(x, y)$, $\boldsymbol{f_0}(y, t)$, $\boldsymbol{f_1}(y, t)$, $\boldsymbol{g_0}(x, t)$ and $\boldsymbol{g_1}(x, t)$ are continuous vector-valued functions.

Let

$$\bar{t}_\sigma = t_\sigma + \frac{k}{2}. \tag{3.5}$$

For $m, n = 0, \pm 1$, define the following approximations in vector form:

$$\overline{\boldsymbol{U}}^{\sigma}_{\beta+m,\varrho+n} = \frac{\boldsymbol{U}^{\sigma+1}_{\beta+m,\varrho+n} + \boldsymbol{U}^{\sigma}_{\beta+m,\varrho+n}}{2}, \tag{3.6}$$

$$\overline{\boldsymbol{U}}^{\sigma}_{x_{\beta,\varrho}} = \frac{\overline{\boldsymbol{U}}^{\sigma}_{\beta+1,\varrho} - \overline{\boldsymbol{U}}^{\sigma}_{\beta-1,\varrho}}{2h}, \tag{3.7}$$

$$\overline{\boldsymbol{U}}^{\sigma}_{y_{\beta,\varrho}} = \frac{\overline{\boldsymbol{U}}^{\sigma}_{\beta,\varrho+1} - \overline{\boldsymbol{U}}^{\sigma}_{\beta,\varrho-1}}{2h}, \tag{3.8}$$

$$\overline{\boldsymbol{U}}^{\sigma}_{t_{\beta,\varrho}} = \frac{\boldsymbol{U}^{\sigma+1}_{\beta,\varrho} - \boldsymbol{U}^{\sigma}_{\beta,\varrho}}{k}, \tag{3.9}$$

$$\overline{\boldsymbol{U}}^{\sigma}_{t_{\beta\pm1,\varrho}} = \frac{\boldsymbol{U}^{\sigma+1}_{\beta\pm1,\varrho} - \boldsymbol{U}^{\sigma}_{\beta\pm1,\varrho}}{k}, \tag{3.10}$$

$$\overline{\boldsymbol{U}}^{\sigma}_{t_{\beta,\varrho\pm1}} = \frac{\boldsymbol{U}^{\sigma+1}_{\beta,\varrho\pm1} - \boldsymbol{U}^{\sigma}_{\beta,\varrho\pm1}}{k}, \tag{3.11}$$

$$\overline{\boldsymbol{U}}^{\sigma}_{x_{\beta\pm1,\varrho}} = \frac{\pm3\overline{\boldsymbol{U}}^{\sigma}_{\beta\pm1,\varrho} \mp 4\overline{\boldsymbol{U}}^{\sigma}_{\beta,\varrho} \pm \overline{\boldsymbol{U}}^{\sigma}_{\beta\mp1,\varrho}}{2h}, \tag{3.12}$$

$$\overline{\boldsymbol{U}}^{\sigma}_{x_{\beta,\varrho\pm1}} = \frac{\overline{\boldsymbol{U}}^{\sigma}_{\beta+1,\varrho\pm1} - \overline{\boldsymbol{U}}^{\sigma}_{\beta-1,\varrho\pm1}}{2h}, \tag{3.13}$$

$$\overline{\boldsymbol{U}}^{\sigma}_{y_{\beta\pm1,\varrho}} = \frac{\overline{\boldsymbol{U}}^{\sigma}_{\beta\pm1,\varrho+1} - \overline{\boldsymbol{U}}^{\sigma}_{\beta\pm1,\varrho-1}}{2h}, \tag{3.14}$$

$$\overline{\boldsymbol{U}}^{\sigma}_{y_{\beta,\varrho\pm1}} = \frac{\pm3\overline{\boldsymbol{U}}^{\sigma}_{\beta,\varrho\pm1} \mp 4\overline{\boldsymbol{U}}^{\sigma}_{\beta,\varrho} \pm \overline{\boldsymbol{U}}^{\sigma}_{\beta,\varrho\mp1}}{2h}, \tag{3.15}$$

$$\overline{\boldsymbol{U}}^{\sigma}_{xx_{\beta,\varrho}} = \frac{\overline{\boldsymbol{U}}^{\sigma}_{\beta+1,\varrho} - 2\overline{\boldsymbol{U}}^{\sigma}_{\beta,\varrho} + \overline{\boldsymbol{U}}^{\sigma}_{\beta-1,\varrho}}{h^2}, \tag{3.16}$$

$$\overline{\boldsymbol{U}}^{\sigma}_{yy_{\beta,\varrho}} = \frac{\overline{\boldsymbol{U}}^{\sigma}_{\beta,\varrho+1} - 2\overline{\boldsymbol{U}}^{\sigma}_{\beta,\varrho} + \overline{\boldsymbol{U}}^{\sigma}_{\beta,\varrho-1}}{h^2}, \tag{3.17}$$

$$\overline{\boldsymbol{U}}^{\sigma}_{xx_{\beta,\varrho\pm1}} = \frac{\overline{\boldsymbol{U}}^{\sigma}_{\beta+1,\varrho\pm1} - 2\overline{\boldsymbol{U}}^{\sigma}_{\beta,\varrho\pm1} + \overline{\boldsymbol{U}}^{\sigma}_{\beta-1,\varrho\pm1}}{h^2}, \tag{3.18}$$

$$\overline{\boldsymbol{U}}^{\sigma}_{yy_{\beta\pm1,\varrho}} = \frac{\overline{\boldsymbol{U}}^{\sigma}_{\beta\pm1,\varrho+1} - 2\overline{\boldsymbol{U}}^{\sigma}_{\beta\pm1,\varrho} + \overline{\boldsymbol{U}}^{\sigma}_{\beta\pm1,\varrho-1}}{h^2}, \tag{3.19}$$

$$\overline{\boldsymbol{U}}^{\sigma}_{xxy_{\beta,\varrho}} = \frac{\overline{\boldsymbol{U}}^{\sigma}_{xx_{\beta,\varrho+1}} - \overline{\boldsymbol{U}}^{\sigma}_{xx_{\beta,\varrho-1}}}{2h}, \tag{3.20}$$

$$\overline{\boldsymbol{U}}^{\sigma}_{xyy_{\beta,\varrho}} = \frac{\overline{\boldsymbol{U}}^{\sigma}_{yy_{\beta+1,\varrho}} - \overline{\boldsymbol{U}}^{\sigma}_{yy_{\beta-1,\varrho}}}{2h}, \tag{3.21}$$

$$\overline{\boldsymbol{U}}^{\sigma}_{xxyy_{\beta,\varrho}} = \frac{\overline{\boldsymbol{U}}^{\sigma}_{xx_{\beta,\varrho+1}} - 2\overline{\boldsymbol{U}}^{\sigma}_{xx_{\beta,\varrho}} + \overline{\boldsymbol{U}}^{\sigma}_{xx_{\beta,\varrho-1}}}{h^2}, \tag{3.22}$$

$$\begin{aligned}\overline{\boldsymbol{F}}^{\sigma}_{\beta\pm1,\varrho} = \boldsymbol{f}\Big(& x_{\beta\pm1}, y_{\varrho}, \bar{t}_{\sigma}, \overline{U}^{(1),\sigma}_{\beta\pm1,\varrho}, \overline{U}^{(2),\sigma}_{\beta\pm1,\varrho}, \ldots, \overline{U}^{(M),\sigma}_{\beta\pm1,\varrho}, \overline{U}^{(1),\sigma}_{x_{\beta\pm1,\varrho}}, \overline{U}^{(2),\sigma}_{x_{\beta\pm1,\varrho}}, \ldots, \overline{U}^{(M),\sigma}_{x_{\beta\pm1,\varrho}},\\ & \overline{U}^{(1),\sigma}_{y_{\beta\pm1,\varrho}}, \overline{U}^{(2),\sigma}_{y_{\beta\pm1,\varrho}}, \ldots, \overline{U}^{(M),\sigma}_{y_{\beta\pm1,\varrho}}, \overline{U}^{(1),\sigma}_{t_{\beta\pm1,\varrho}}, \overline{U}^{(2),\sigma}_{t_{\beta\pm1,\varrho}}, \ldots, \overline{U}^{(M),\sigma}_{t_{\beta\pm1,\varrho}}\Big),\end{aligned} \tag{3.23}$$

$$\begin{aligned}\overline{\boldsymbol{F}}^{\sigma}_{\beta,\varrho\pm1} = \boldsymbol{f}\Big(& x_{\beta}, y_{\varrho\pm1}, \bar{t}_{\sigma}, \overline{U}^{(1),\sigma}_{\beta,\varrho\pm1}, \overline{U}^{(2),\sigma}_{\beta,\varrho\pm1}, \ldots, \overline{U}^{(M),\sigma}_{\beta,\varrho\pm1}, \overline{U}^{(1),\sigma}_{x_{\beta,\varrho\pm1}}, \overline{U}^{(2),\sigma}_{x_{\beta,\varrho\pm1}}, \ldots, \overline{U}^{(M),\sigma}_{x_{\beta,\varrho\pm1}},\\ & \overline{U}^{(1),\sigma}_{y_{\beta,\varrho\pm1}}, \overline{U}^{(2),\sigma}_{y_{\beta,\varrho\pm1}}, \ldots, \overline{U}^{(M),\sigma}_{y_{\beta,\varrho\pm1}}, \overline{U}^{(1),\sigma}_{t_{\beta,\varrho\pm1}}, \overline{U}^{(2),\sigma}_{t_{\beta,\varrho\pm1}}, \ldots, \overline{U}^{(M),\sigma}_{t_{\beta,\varrho\pm1}}\Big),\end{aligned} \tag{3.24}$$

$$\begin{aligned}\overline{\overline{\boldsymbol{F}}}^{\sigma}_{\beta,\varrho} = \boldsymbol{f}\Big(& x_{\beta}, y_{\varrho}, \bar{t}_{\sigma}, \overline{U}^{(1),\sigma}_{\beta,\varrho}, \overline{U}^{(2),\sigma}_{\beta,\varrho}, \ldots, \overline{U}^{(M),\sigma}_{\beta,\varrho}, \overline{\overline{U}}^{(1),\sigma}_{x_{\beta,\varrho}}, \overline{\overline{U}}^{(2),\sigma}_{x_{\beta,\varrho}}, \ldots, \overline{\overline{U}}^{(M),\sigma}_{x_{\beta,\varrho}},\\ & \overline{\overline{U}}^{(1),\sigma}_{y_{\beta,\varrho}}, \overline{\overline{U}}^{(2),\sigma}_{y_{\beta,\varrho}}, \ldots, \overline{\overline{U}}^{(M),\sigma}_{y_{\beta,\varrho}}, \overline{U}^{(1),\sigma}_{t_{\beta,\varrho}}, \overline{U}^{(2),\sigma}_{t_{\beta,\varrho}}, \ldots, \overline{U}^{(M),\sigma}_{t_{\beta,\varrho}}\Big),\end{aligned} \tag{3.25}$$

where

$$\begin{aligned}\overline{\overline{\boldsymbol{U}}}^{\sigma}_{x_{\beta,\varrho}} = \overline{\boldsymbol{U}}^{\sigma}_{x_{\beta,\varrho}} - \frac{h}{12\boldsymbol{A}^{\sigma}_{\beta,\varrho}}\left(\overline{\boldsymbol{F}}^{\sigma}_{\beta+1,\varrho} - \overline{\boldsymbol{F}}^{\sigma}_{\beta-1,\varrho}\right) + \frac{h^2\boldsymbol{C}^{\sigma}_{\beta,\varrho}}{6\boldsymbol{A}^{\sigma}_{\beta,\varrho}}\overline{\boldsymbol{U}}^{\sigma}_{xyy_{\beta,\varrho}}\\ + 2h^2\left(\frac{\boldsymbol{A}^{\sigma}_{x_{\beta,\varrho}}}{12\boldsymbol{A}^{\sigma}_{\beta,\varrho}}\overline{\boldsymbol{U}}^{\sigma}_{xx_{\beta,\varrho}} + \frac{\boldsymbol{C}^{\sigma}_{x_{\beta,\varrho}}}{12\boldsymbol{A}^{\sigma}_{\beta,\varrho}}\overline{\boldsymbol{U}}^{\sigma}_{yy_{\beta,\varrho}}\right),\end{aligned}$$

$$\begin{aligned}\overline{\overline{\boldsymbol{U}}}^{\sigma}_{y_{\beta,\varrho}} = \overline{\boldsymbol{U}}^{\sigma}_{y_{\beta,\varrho}} - \frac{h}{12\boldsymbol{C}^{\sigma}_{\beta,\varrho}}\left(\overline{\boldsymbol{F}}^{\sigma}_{\beta,\varrho+1} - \overline{\boldsymbol{F}}^{\sigma}_{\beta,\varrho-1}\right) + \frac{h^2\boldsymbol{A}^{\sigma}_{\beta,\varrho}}{6\boldsymbol{C}^{\sigma}_{\beta,\varrho}}\overline{\boldsymbol{U}}^{\sigma}_{xxy_{\beta,\varrho}}\\ + 2h^2\left(\frac{\boldsymbol{A}^{\sigma}_{y_{\beta,\varrho}}}{12\boldsymbol{C}^{\sigma}_{\beta,\varrho}}\overline{\boldsymbol{U}}^{\sigma}_{xx_{\beta,\varrho}} + \frac{\boldsymbol{C}^{\sigma}_{y_{\beta,\varrho}}}{12\boldsymbol{C}^{\sigma}_{\beta,\varrho}}\overline{\boldsymbol{U}}^{\sigma}_{yy_{\beta,\varrho}}\right).\end{aligned}$$

Further, we define the following additional functional approximation as:

$$\widehat{\widehat{\boldsymbol{F}}}^{\sigma}_{\beta,\varrho} = \boldsymbol{f}\Big(x_\beta, y_\varrho, \bar{t}_\sigma, \overline{\boldsymbol{U}}^{(1),\sigma}_{\beta,\varrho}, \overline{\boldsymbol{U}}^{(2),\sigma}_{\beta,\varrho}, \ldots, \overline{\boldsymbol{U}}^{(M),\sigma}_{\beta,\varrho}, \widehat{\widehat{\boldsymbol{U}}}^{(1),\sigma}_{x_{\beta,\varrho}}, \widehat{\widehat{\boldsymbol{U}}}^{(2),\sigma}_{x_{\beta,\varrho}}, \ldots, \widehat{\widehat{\boldsymbol{U}}}^{(M),\sigma}_{x_{\beta,\varrho}},$$
$$\widehat{\widehat{\boldsymbol{U}}}^{(1),\sigma}_{y_{\beta,\varrho}}, \widehat{\widehat{\boldsymbol{U}}}^{(2),\sigma}_{y_{\beta,\varrho}}, \ldots, \widehat{\widehat{\boldsymbol{U}}}^{(M),\sigma}_{y_{\beta,\varrho}}, \overline{\boldsymbol{U}}^{(1),\sigma}_{t_{\beta,\varrho}}, \overline{\boldsymbol{U}}^{(2),\sigma}_{t_{\beta,\varrho}}, \ldots, \overline{\boldsymbol{U}}^{(M),\sigma}_{t_{\beta,\varrho}}\Big), \tag{3.26}$$

where

$$\widehat{\widehat{\boldsymbol{U}}}^{\sigma}_{x_{\beta,\varrho}} = \overline{\boldsymbol{U}}^{\sigma}_{x_{\beta,\varrho}} - \frac{h}{8\boldsymbol{A}^{\sigma}_{\beta,\varrho}}\left(\overline{\boldsymbol{F}}^{\sigma}_{\beta+1,\varrho} - \overline{\boldsymbol{F}}^{\sigma}_{\beta-1,\varrho}\right) + \frac{h^2\boldsymbol{C}^{\sigma}_{\beta,\varrho}}{4\boldsymbol{A}^{\sigma}_{\beta,\varrho}}\overline{\boldsymbol{U}}^{\sigma}_{xyy_{\beta,\varrho}} + 2h^2\left(\frac{\boldsymbol{A}^{\sigma}_{x_{\beta,\varrho}}}{8\boldsymbol{A}^{\sigma}_{\beta,\varrho}}\overline{\boldsymbol{U}}^{\sigma}_{xx_{\beta,\varrho}} + \frac{\boldsymbol{C}^{\sigma}_{x_{\beta,\varrho}}}{8\boldsymbol{A}^{\sigma}_{\beta,\varrho}}\overline{\boldsymbol{U}}^{\sigma}_{yy_{\beta,\varrho}}\right),$$

$$\widehat{\widehat{\boldsymbol{U}}}^{\sigma}_{y_{\beta,\varrho}} = \overline{\boldsymbol{U}}^{\sigma}_{y_{\beta,\varrho}} - \frac{h}{8\boldsymbol{C}^{\sigma}_{\beta,\varrho}}\left(\overline{\boldsymbol{F}}^{\sigma}_{\beta,\varrho+1} - \overline{\boldsymbol{F}}^{\sigma}_{\beta,\varrho-1}\right) + \frac{h^2\boldsymbol{A}^{\sigma}_{\beta,\varrho}}{4\boldsymbol{C}^{\sigma}_{\beta,\varrho}}\overline{\boldsymbol{U}}^{\sigma}_{xxy_{\beta,\varrho}} + 2h^2\left(\frac{\boldsymbol{A}^{\sigma}_{y_{\beta,\varrho}}}{8\boldsymbol{C}^{\sigma}_{\beta,\varrho}}\overline{\boldsymbol{U}}^{\sigma}_{xx_{\beta,\varrho}} + \frac{\boldsymbol{C}^{\sigma}_{y_{\beta,\varrho}}}{8\boldsymbol{C}^{\sigma}_{\beta,\varrho}}\overline{\boldsymbol{U}}^{\sigma}_{yy_{\beta,\varrho}}\right).$$

Now, the system of PDEs (3.1) at each interior nodal point $\left(x_\beta, y_\varrho, t_\sigma\right)$ may be approximated in exponential-vector form as:

$$\begin{aligned}\boldsymbol{L}\left[\overline{\boldsymbol{U}}\right] &= \left[\overline{\boldsymbol{L}}_1\overline{\boldsymbol{U}}^{\sigma}_{xx_{\beta,\varrho}} + \overline{\boldsymbol{L}}_2\overline{\boldsymbol{U}}^{\sigma}_{yy_{\beta,\varrho}} + \overline{\boldsymbol{L}}_3\overline{\boldsymbol{U}}^{\sigma}_{xxy_{\beta,\varrho}} + \overline{\boldsymbol{L}}_4\overline{\boldsymbol{U}}^{\sigma}_{xyy_{\beta,\varrho}} + \overline{\boldsymbol{L}}_5\overline{\boldsymbol{U}}^{\sigma}_{xxyy_{\beta,\varrho}}\right]\\ &= \overline{\overline{\boldsymbol{F}}}^{\sigma}_{\beta,\varrho}\exp\left(\frac{\overline{\boldsymbol{J}}_1\overline{\boldsymbol{F}}^{\sigma}_{\beta+1,\varrho} + \overline{\boldsymbol{J}}_2\overline{\boldsymbol{F}}^{\sigma}_{\beta-1,\varrho} + \overline{\boldsymbol{J}}_3\overline{\boldsymbol{F}}^{\sigma}_{\beta,\varrho+1} + \overline{\boldsymbol{J}}_4\overline{\boldsymbol{F}}^{\sigma}_{\beta,\varrho-1} - 4\widehat{\widehat{\boldsymbol{F}}}^{\sigma}_{\beta,\varrho}}{12\overline{\overline{\boldsymbol{F}}}^{\sigma}_{\beta,\varrho}}\right) + \overline{\boldsymbol{T}}^{\sigma}_{\beta,\varrho},\end{aligned} \tag{3.27}$$

where $\overline{\boldsymbol{L}}_1 = \overline{\boldsymbol{A}}^{\sigma}_{\beta,\varrho} + \frac{h^2}{12}\left(\overline{\boldsymbol{A}}^{\sigma}_{xx_{\beta,\varrho}} + \overline{\boldsymbol{A}}^{\sigma}_{yy_{\beta,\varrho}}\right) - \left(\frac{h\overline{\boldsymbol{A}}^{\sigma}_{x_{\beta,\varrho}}}{6\overline{\boldsymbol{A}}^{\sigma}_{\beta,\varrho}}\right)h\overline{\boldsymbol{A}}^{\sigma}_{x_{\beta,\varrho}} - \left(\frac{h\overline{\boldsymbol{C}}^{\sigma}_{y_{\beta,\varrho}}}{6\overline{\boldsymbol{C}}^{\sigma}_{\beta,\varrho}}\right)h\overline{\boldsymbol{A}}^{\sigma}_{y_{\beta,\varrho}}$,

$\overline{\boldsymbol{L}}_2 = \overline{\boldsymbol{C}}^{\sigma}_{\beta,\varrho} + \frac{h^2}{12}\left(\overline{\boldsymbol{C}}^{\sigma}_{xx_{\beta,\varrho}} + \overline{\boldsymbol{C}}^{\sigma}_{yy_{\beta,\varrho}}\right) - \left(\frac{h\overline{\boldsymbol{A}}^{\sigma}_{x_{\beta,\varrho}}}{6\overline{\boldsymbol{A}}^{\sigma}_{\beta,\varrho}}\right)h\overline{\boldsymbol{C}}^{\sigma}_{x_{\beta,\varrho}} - \left(\frac{h\overline{\boldsymbol{C}}^{\sigma}_{y_{\beta,\varrho}}}{6\overline{\boldsymbol{C}}^{\sigma}_{\beta,\varrho}}\right)h\overline{\boldsymbol{C}}^{\sigma}_{y_{\beta,\varrho}}$,

$\overline{\boldsymbol{L}}_3 = \frac{h^2}{6}\left[\overline{\boldsymbol{A}}^{\sigma}_{y_{\beta,\varrho}} - \frac{\overline{\boldsymbol{C}}^{\sigma}_{y_{\beta,\varrho}}}{\overline{\boldsymbol{C}}^{\sigma}_{\beta,\varrho}}\overline{\boldsymbol{A}}^{\sigma}_{\beta,\varrho}\right]$, $\overline{\boldsymbol{L}}_4 = \frac{h^2}{6}\left[\overline{\boldsymbol{C}}^{\sigma}_{x_{\beta,\varrho}} - \frac{\overline{\boldsymbol{A}}^{\sigma}_{x_{\beta,\varrho}}}{\overline{\boldsymbol{A}}^{\sigma}_{\beta,\varrho}}\overline{\boldsymbol{C}}^{\sigma}_{\beta,\varrho}\right]$, $\overline{\boldsymbol{L}}_5 = h^2\left[\frac{\overline{\boldsymbol{A}}^{\sigma}_{\beta,\varrho} + \overline{\boldsymbol{C}}^{\sigma}_{\beta,\varrho}}{12}\right]$, and

$\overline{\boldsymbol{J}}_1 = 1 - h\frac{\overline{\boldsymbol{A}}^{\sigma}_{x_{\beta,\varrho}}}{\overline{\boldsymbol{A}}^{\sigma}_{\beta,\varrho}}$, $\overline{\boldsymbol{J}}_2 = 1 + h\frac{\overline{\boldsymbol{A}}^{\sigma}_{x_{\beta,\varrho}}}{\overline{\boldsymbol{A}}^{\sigma}_{\beta,\varrho}}$, $\overline{\boldsymbol{J}}_3 = 1 - h\frac{\overline{\boldsymbol{C}}^{\sigma}_{y_{\beta,\varrho}}}{\overline{\boldsymbol{C}}^{\sigma}_{\beta,\varrho}}$, $\overline{\boldsymbol{J}}_4 = 1 + h\frac{\overline{\boldsymbol{C}}^{\sigma}_{y_{\beta,\varrho}}}{\overline{\boldsymbol{C}}^{\sigma}_{\beta,\varrho}}$,

and $\overline{\boldsymbol{T}}^{\sigma}_{\beta,\varrho} = O\left(k^2 + kh^2 + h^4\right)$.

The next one in our study is the fourth-order IBVP (1.5)-(1.7). We introduce a new variable v as:

$$\nabla^2 u = v, \qquad (x, y, t) \in \Omega_2 \tag{3.28}$$

Then, the equation (1.5) is reduced to

$$A\left(x, y, t\right)\nabla^2 v = g\left(x, y, t, u, u_x, u_y, v, v_x, v_y\right) - u_t, \qquad (x, y, t) \in \Omega_2 \tag{3.29}$$

On applying the proposed method (2.57) to coupled equation (3.28)-(3.29), we obtain:

$$\left[\overline{U}^{\sigma}_{xx_{\beta,\varrho}}+\overline{U}^{\sigma}_{yy_{\beta,\varrho}}+\frac{h^2}{6}\overline{U}^{\sigma}_{xxyy_{\beta,\varrho}}\right]$$
$$=\overline{V}^{\sigma}_{\beta,\varrho}\exp\left(\frac{\overline{V}^{\sigma}_{\beta+1,\varrho}+\overline{V}^{\sigma}_{\beta-1,\varrho}+\overline{V}^{\sigma}_{\beta,\varrho+1}+\overline{V}^{\sigma}_{\beta,\varrho-1}-4\overline{V}^{\sigma}_{\beta,\varrho}}{12\overline{V}^{\sigma}_{\beta,\varrho}}\right)+\overline{T}^{(1),\sigma}_{\beta,\varrho}, \tag{3.30}$$

$$\left[\overline{L}_1\overline{V}^{\sigma}_{xx_{\beta,\varrho}}+\overline{L}_2\overline{V}^{\sigma}_{yy_{\beta,\varrho}}+\overline{L}_5\overline{V}^{\sigma}_{xxyy_{\beta,\varrho}}\right]$$
$$=\overline{\overline{G}}^{\sigma}_{\beta,\varrho}\exp\left(\frac{\overline{J}_1\overline{G}^{\sigma}_{\beta+1,\varrho}+\overline{J}_2\overline{G}^{\sigma}_{\beta-1,\varrho}+\overline{J}_3\overline{G}^{\sigma}_{\beta,\varrho+1}+\overline{J}_4\overline{G}^{\sigma}_{\beta,\varrho-1}-4\widehat{\widehat{G}}^{\sigma}_{\beta,\varrho}}{12\overline{\overline{G}}^{\sigma}_{\beta,\varrho}}\right)$$
$$-\overline{U}^{\sigma}_{t_{\beta,\varrho}}\exp\left(\frac{\overline{J}_1\overline{U}^{\sigma}_{t_{\beta+1,\varrho}}+\overline{J}_2\overline{U}^{\sigma}_{t_{\beta-1,\varrho}}+\overline{J}_3\overline{U}^{\sigma}_{t_{\beta,\varrho+1}}+\overline{J}_4\overline{U}^{\sigma}_{t_{\beta,\varrho-1}}-4\overline{U}^{\sigma}_{t_{\beta,\varrho}}}{12\overline{U}^{\sigma}_{t_{\beta,\varrho}}}\right)+\overline{T}^{(2),\sigma}_{\beta,\varrho}, \tag{3.31}$$

where $G^{\sigma}_{\beta,\varrho}=g(x_\beta,y_\varrho,t_\sigma,U^{\sigma}_{\beta,\varrho},U^{\sigma}_{x\beta,\varrho},U^{\sigma}_{y\beta,\varrho},V^{\sigma}_{\beta,\varrho},V^{\sigma}_{x\beta,\varrho},V^{\sigma}_{y\beta,\varrho})$, $\overline{T}^{(1),\sigma}_{\beta,\varrho}=\left(k^2+kh^2+h^4\right)$ and $\overline{T}^{(2),\sigma}_{\beta,\varrho}=O\left(k^2+kh^2+h^4\right)$.

It should be noted that on the boundary of $0<x,y<a$, the values of the variables u,u_{xx},u_{yy} are described and this implies that u and v can be prescribed on this boundary. With the aid of initial condition $u(x,y,0)$, we can compute the system of equations (3.30)-(3.31) using suitable iteration methods [25].

4 Consideration of the ADI scheme and stability analysis

For stability, we consider the following two-dimensional singular PPDE:

$$u_{xx}+u_{yy}+D(x)u_x=u_t+s\left(x,y,t\right),\qquad (x,y,t)\in\Omega_2, \tag{4.1}$$

where $D(x)=\frac{1}{x}$. In this case, $F=-D(x)u_x+u_t+s\left(x,y,t\right)$.

By using the difference method (2.57) to solve the PPDE (4.1), we reach the following result:

$$
\begin{aligned}
&\left[\overline{U}^{\sigma}_{xx_{\beta,\varrho}} + \overline{U}^{\sigma}_{yy_{\beta,\varrho}} + \frac{h^2}{6}\overline{U}^{\sigma}_{xxyy_{\beta,\varrho}}\right] \\
&= \overline{\overline{F}}^{\sigma}_{\beta,\varrho} \exp\left(\frac{\overline{F}^{\sigma}_{\beta+1,\varrho} + \overline{F}^{\sigma}_{\beta-1,\varrho} + \overline{F}^{\sigma}_{\beta,\varrho+1} + \overline{F}^{\sigma}_{\beta,\varrho-1} - 4\widehat{\overline{F}}^{\sigma}_{\beta,\varrho}}{12\overline{\overline{F}}^{\sigma}_{\beta,\varrho}}\right) + O\left(k^2 + kh^2 + h^4\right)
\end{aligned}
\tag{4.2}
$$

where

$$
\begin{aligned}
\overline{F}^{\sigma}_{\beta\pm1,\varrho} &= -D_{\beta\pm1}\overline{U}^{\sigma}_{x_{\beta\pm1,\varrho}} + \overline{U}^{\sigma}_{t_{\beta\pm1,\varrho}} + \overline{s}^{\sigma}_{\beta\pm1,\varrho}, \\
\overline{F}^{\sigma}_{\beta,\varrho\pm1} &= -D_{\beta}\overline{U}^{\sigma}_{x_{\beta,\varrho\pm1}} + \overline{U}^{\sigma}_{t_{\beta,\varrho\pm1}} + \overline{s}^{\sigma}_{\beta,\varrho\pm1}, \\
\overline{\overline{F}}^{\sigma}_{\beta,\varrho} &= -D_{\beta}\overline{\overline{U}}^{\sigma}_{x_{\beta,\varrho}} + \overline{U}^{\sigma}_{t_{\beta,\varrho}} + \overline{s}^{\sigma}_{\beta,\varrho}, \\
\widehat{\overline{F}}^{\sigma}_{\beta,\varrho} &= -D_{\beta}\widehat{\overline{U}}^{\sigma}_{x_{\beta,\varrho}} + \overline{U}^{\sigma}_{t_{\beta,\varrho}} + \overline{s}^{\sigma}_{\beta,\varrho}.
\end{aligned}
$$

Note that $D_{\beta-1} = \dfrac{-1}{x_{\beta-1}}$ can't be evaluated at $\beta = 1$, since $x_0 = 0$ is a singular point. We overcome this difficulty by modifying the scheme (4.2) in such a way that the solution retains its order and accuracy everywhere in the solution region including in the vicinity of the singularity. For this purpose, we need the following approximations:

$$
D_{\beta\pm1} = D_{\beta} \pm hD_{x_\beta} + \frac{h^2}{2}D_{xx_\beta} \pm O(h^3), \tag{4.3}
$$

$$
\overline{s}^{\sigma}_{\beta\pm1,\varrho} = \overline{s}^{\sigma}_{\beta,\varrho} \pm h\overline{s}^{\sigma}_{x_{\beta,\varrho}} + \frac{h^2}{2}\overline{s}^{\sigma}_{xx_{\beta,\varrho}} \pm O(h^3), \tag{4.4}
$$

$$
\overline{s}^{\sigma}_{\beta,\varrho\pm1} = \overline{s}^{\sigma}_{\beta,\varrho} \pm h\overline{s}^{\sigma}_{y_{\beta,\varrho}} + \frac{h^2}{2}\overline{s}^{\sigma}_{yy_{\beta,\varrho}} \pm O(h^3). \tag{4.5}
$$

Simplifying (4.2) with the assist of the approximations (4.3)-(4.5), the operator form of the equation (4.2) is as follows:

$$
\begin{aligned}
&\Bigg[1 + \frac{1}{12}\left(1 - 6\lambda - \frac{\lambda h^2}{2}\left(2D_x + D^2\right)\right)\delta_x^2 + \frac{1}{12}\left(1 - 6\lambda\right)\delta_y^2 \\
&+ \frac{1}{12}\left(\frac{hD}{2} - \frac{h\lambda}{4}\left(12D + h^2\left(D_{xx} + DD_x\right)\right)\right)(2\mu_x\delta_x) - \frac{\lambda hD}{24}(2\delta_y^2\mu_x\delta_x) - \frac{\lambda}{12}\delta_x^2\delta_y^2\Bigg] U^{\sigma+1}_{\beta,\varrho} \\
&= \Bigg[1 + \frac{1}{12}\left(1 + 6\lambda + \frac{\lambda h^2}{2}\left(2D_x + D^2\right)\right)\delta_x^2 + \frac{1}{12}\left(1 + 6\lambda\right)\delta_y^2 \\
&+ \frac{1}{12}\left(\frac{hD}{2} + \frac{h\lambda}{4}\left(12D + h^2\left(D_{xx} + DD_x\right)\right)\right)(2\mu_x\delta_x) + \frac{\lambda hD}{24}(2\delta_y^2\mu_x\delta_x) + \frac{\lambda}{12}\delta_x^2\delta_y^2\Bigg] U^{\sigma}_{\beta,\varrho} \\
&+ \Sigma s + O\left(k^3 + k^2h^2 + kh^4\right),
\end{aligned}
\tag{4.6}
$$

where δ_x and μ_x are the central difference and average operators, respectively, $\lambda = k/h^2$, and

$D = D(x_\beta), \overline{s} = s\left(x_\beta, y_\varrho, \overline{t}_\sigma\right), \overline{s}_x = s_x\left(x_\beta, y_\varrho, \overline{t}_\sigma\right)$, etc., and $\Sigma s = -\frac{k}{12}\left[12\overline{s} + h^2\left(\overline{s}_{xx} + \overline{s}_{yy} + D\overline{s}_x\right)\right]$.

Neglecting the LTE in (4.6), a two-level implicit scheme, which is consistent with (4.1) can be written as:

$$\begin{aligned}
&\left[1 + \frac{1}{12}\left(1 - 6\lambda - \frac{\lambda h^2}{2}(2D_x + D^2)\right)\delta_x^2 + \frac{1}{12}(1 - 6\lambda)\delta_y^2\right.\\
&\left.+ \frac{1}{12}\left(\frac{hD}{2} - \frac{h\lambda}{4}\left(12D + h^2\left(D_{xx} + DD_x\right)\right)\right)(2\mu_x\delta_x) - \frac{\lambda hD}{24}(2\delta_y^2\mu_x\delta_x) - \frac{\lambda}{12}\delta_x^2\delta_y^2\right] u_{\beta,\varrho}^{\sigma+1}\\
&= \left[1 + \frac{1}{12}\left(1 + 6\lambda + \frac{\lambda h^2}{2}(2D_x + D^2)\right)\delta_x^2 + \frac{1}{12}(1 + 6\lambda)\delta_y^2\right.\\
&\left.+ \frac{1}{12}\left(\frac{hD}{2} + \frac{h\lambda}{4}\left(12D + h^2\left(D_{xx} + DD_x\right)\right)\right)(2\mu_x\delta_x) + \frac{\lambda hD}{24}(2\delta_y^2\mu_x\delta_x) + \frac{\lambda}{12}\delta_x^2\delta_y^2\right] u_{\beta,\varrho}^{\sigma} + \Sigma s.
\end{aligned} \tag{4.7}$$

The scheme (4.7) may be restated in its product form as:

$$[X_1]\,[Y_1]\; u_{\beta,\varrho}^{\sigma+1} = [X_2]\,[Y_2]\; u_{\beta,\varrho}^{\sigma} + \Sigma s, \tag{4.8}$$

where

$$X_1 = \left[1 + \frac{1}{12}\left(1 - 6\lambda - \frac{\lambda h^2}{2}(2D_x + D^2)\right)\delta_x^2 + \frac{1}{12}\left(\frac{hD}{2} - \frac{h\lambda}{4}\left(12D + h^2\left(D_{xx} + DD_x\right)\right)\right)(2\mu_x\delta_x)\right],$$

$$Y_1 = \left[1 + \frac{1}{12}(1 - 6\lambda)\delta_y^2\right],$$

$$X_2 = \left[1 + \frac{1}{12}\left(1 + 6\lambda + \frac{\lambda h^2}{2}(2D_x + D^2)\right)\delta_x^2 + \frac{1}{12}\left(\frac{hD}{2} + \frac{h\lambda}{4}\left(12D + h^2\left(D_{xx} + DD_x\right)\right)\right)(2\mu_x\delta_x)\right],$$

$$Y_2 = \left[1 + \frac{1}{12}(1 + 6\lambda)\delta_y^2\right].$$

Several additional terms in equation (4.8) are of higher-order phenomena that allow the equation (4.7) to be expressed in factorization form without compromising the accuracy of scheme. The ADI form of the method (4.7) looks like this:

$$[Y_1]\,u_{\beta,\varrho}^{*} = [X_2]\,[Y_2]\,u_{\beta,\varrho}^{\sigma} + \Sigma s, \tag{4.9}$$

$$[X_1]\,u_{\beta,\varrho}^{\sigma+1} = u_{\beta,\varrho}^{*}, \tag{4.10}$$

where $u^*_{\beta,\varrho}$ is an intermediate vector and using the equation (4.10), we can get the intermediate boundary conditions.

Assume that $\epsilon^\sigma_{\beta,\varrho} = U^\sigma_{\beta,\varrho} - u^\sigma_{\beta,\varrho}$ be the error at each interior grid point. Subtracting (4.7) from (4.6), we get the error equation

$$
\begin{aligned}
&\Bigg[1 + \frac{1}{12}\Big(1 - 6\lambda - \frac{\lambda h^2}{2}(2D_x + D^2)\Big)\delta_x^2 + \frac{1}{12}(1 - 6\lambda)\delta_y^2 \\
&+ \frac{1}{12}\left(\frac{hD}{2} - \frac{h\lambda}{4}\Big(12D + h^2\big(D_{xx} + DD_x\big)\Big)\right)(2\mu_x\delta_x) - \frac{\lambda hD}{24}(2\delta_y^2\mu_x\delta_x) - \frac{\lambda}{12}\delta_x^2\delta_y^2\Bigg]\,\epsilon^{\sigma+1}_{\beta,\varrho} \\
&\qquad = \Bigg[1 + \frac{1}{12}\Big(1 + 6\lambda + \frac{\lambda h^2}{2}(2D_x + D^2)\Big)\delta_x^2 + \frac{1}{12}(1 + 6\lambda)\delta_y^2 \\
&+ \frac{1}{12}\left(\frac{hD}{2} + \frac{h\lambda}{4}\Big(12D + h^2\big(D_{xx} + DD_x\big)\Big)\right)(2\mu_x\delta_x) + \frac{\lambda hD}{24}(2\delta_y^2\mu_x\delta_x) + \frac{\lambda}{12}\delta_x^2\delta_y^2\Bigg]\,\epsilon^{\sigma}_{\beta,\varrho} \\
&\qquad\qquad + O\left(k^3 + k^2h^2 + kh^4\right),
\end{aligned}
$$

which in product form can be written as:

$$
[X_1]\,[Y_1]\ \epsilon^{\sigma+1}_{\beta,\varrho} = [X_2]\,[Y_2]\ \epsilon^{\sigma}_{\beta,\varrho} + O\left(k^3 + k^2h^2 + kh^4\right). \tag{4.11}
$$

For analyzing stability, we assume that the error is of the form $\epsilon^\sigma_{\beta,\varrho} = \xi^\sigma e^{i(\theta_x\beta + \theta_y\varrho)}$ which exists at each grid point, where ξ is the amplification factor, $i = \sqrt{-1}$ and θ_x, θ_y are the real angles. Discarding the LTE and substituting $\epsilon^\sigma_{\beta,\varrho}$ in the error equation (4.11), we can express the characteristic equation as:

$$
\xi = \xi_x . \xi_y, \tag{4.12}
$$

where

$$
\begin{aligned}
\xi_x &= \frac{\left[1 + \frac{1}{6}\Big(1 + 6\lambda + \frac{\lambda h^2}{2}(2D_x + D^2)\Big)(\cos\theta_x - 1) + \frac{i}{6}\left(\frac{hD}{2} + \frac{h\lambda}{4}\Big(12D + h^2\big(D_{xx} + DD_x\big)\Big)\right)\sin\theta_x\right]}{\left[1 + \frac{1}{6}\Big(1 - 6\lambda - \frac{\lambda h^2}{2}(2D_x + D^2)\Big)(\cos\theta_x - 1) + \frac{i}{6}\left(\frac{hD}{2} - \frac{h\lambda}{4}\Big(12D + h^2\big(D_{xx} + DD_x\big)\Big)\right)\sin\theta_x\right]} \\
&= \frac{1 + \lambda L(\theta_x)}{1 - \lambda L(\theta_x)}.
\end{aligned}
$$

Here,

$$
\begin{aligned}
L(\theta_x) &= \frac{\Big(6 + \frac{h^2}{2}(2D_x + D^2)\Big)\big(\cos\theta_x - 1\big) + \frac{ih}{4}\Big(12D + h^2\big(D_{xx} + DD_x\big)\Big)\sin\theta_x}{\Big(5 + \cos\theta_x + \frac{ihD}{2}\sin\theta_x\Big)} \\
&= p + iq,
\end{aligned} \tag{4.13}
$$

where $p = Re(L(\theta_x))$. So, we have

$$\xi_x = \frac{1 + \lambda(p + iq)}{1 - \lambda(p + iq)} = \frac{(1 + \lambda p) + i\lambda q}{(1 - \lambda p) - i\lambda q}.$$

Assume that the initial error $\epsilon^0_{\beta,\varrho}$ shall not grow as $\sigma \to \infty$. The numerical method (4.8) to be stable [59], it is necessary and sufficient that $|\xi| \le 1$.

It is easy to corroborate that $|\xi_x| \le 1$, i.e. $Re(L(\theta_x)) \le 0$ and it is true for $D = \frac{1}{x}$ here. In a similar manner, we can show that $\left|\xi_y\right| \le 1$.

Thus, from (4.12), we conclude that

$$|\xi| = |\xi_x| \, . \left|\xi_y\right| \le 1.$$

Hence, the scheme (4.8) is unconditionally stable ($0 < \lambda < \infty$) for the linear equation (4.1).

Since the method (4.8) is a two-level implicit in nature, stable and consistent, the method (4.8) is convergent.

5 Computational results

Here, we demonstrate the efficiency of the suggested technique by presenting the outcomes of certain numerical experiments implemented on a variety of quasi-linear problems. The analytical solutions to the problems are provided as part of the testing process. The analytical solutions may be used to derive the forcing function of the problem as well as the initial and boundary conditions. For the system of quasi-linear difference equations, Newton's non-linear block iteration technique is utilised [25]. The error tolerance for the end of the iteration is set to 10^{-15}, and the first estimate is predicted to be trivial, i.e. **u=0**. We have used an Intel CORE i7-11700F processor for numerical computations. The system includes 16GB of RAM. All calculations were performed using MATLAB R2024a. The operating system is Windows 11 Pro. We did not use additional hardware or other software beyond MATLAB and its standard toolboxes. The maximum absolute errors (MAEs) are computed for all the numerical problems which is defined as:

$$\text{MAEs} = \max_{\substack{\beta=1(1)l,\varrho=1(1)m,\\ \sigma=1(1)j}} \left| U^{\sigma}_{\beta,\varrho} - u^{\sigma}_{\beta,\varrho} \right|.$$

The spatial rate of convergence ρ_h is also tabulated which is computed by:

$$\rho_h = \frac{\log(e_{h_{x_1}}/e_{h_{x_2}})}{\log(h_{x_1}/h_{x_2})}, \tag{5.1}$$

Table 1 MAEs at $t = 1$ for Example 1

h	Proposed Scheme (4.9)-(4.10)				Method discussed in [35]			
	$\gamma = 1$	$\gamma = 2$	ρ_h	ρ_k	$\gamma = 1$	$\gamma = 2$	ρ_h	ρ_k
$\frac{1}{16}$	1.9124e−07	2.2804e−07	–	–	3.9471e−07	4.8426e−07	–	–
$\frac{1}{32}$	1.2035e−08	1.4217e−08	4.0036	2.0018	2.2856e−08	3.0285e−08	3.9991	1.9996
$\frac{1}{64}$	7.5611e−10	8.8541e−10	4.0051	2.0026	1.4140e−09	1.8930e−09	3.9998	1.9999

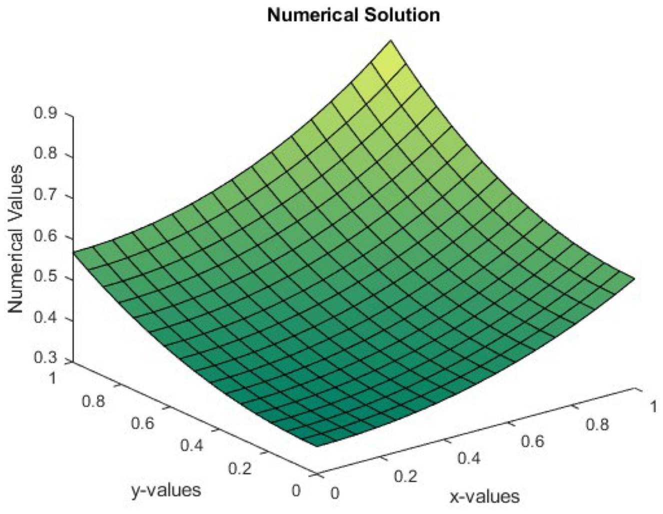

(a): Numerical Solutions with $h = \frac{1}{16}, \gamma = 1$ at $t = 1$ for Example 1

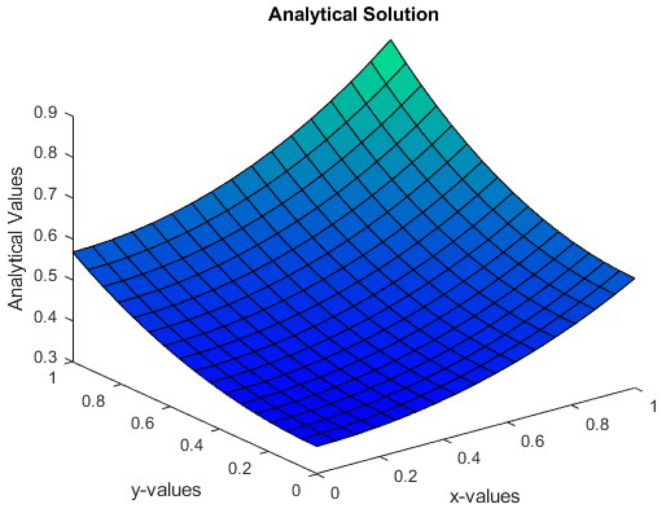

(b): Analytical Solutions with $h = \frac{1}{16}, \gamma = 1$ at $t = 1$ for Example 1

Fig. 1 (a) Numerical Solutions with $h = \frac{1}{16}, \gamma = 1$ at $t = 1$ for Example 1. (b) Analytical Solutions with $h = \frac{1}{16}, \gamma = 1$ at $t = 1$ for Example 1. (c) log-log error plot with $\gamma = 1, 2$ for Example 1. (d) log-log error plot with $\gamma = 1, 2$ for Example 1

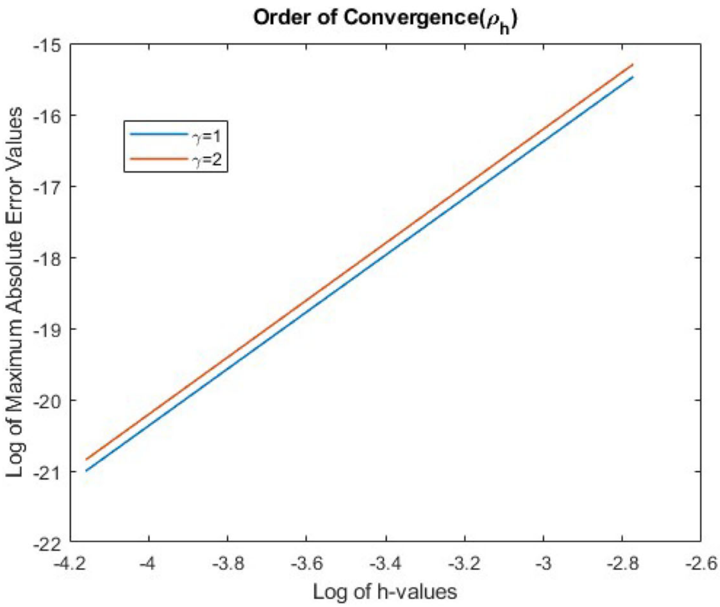

(c): log-log error plot with $\gamma = 1, 2$ for Example 1

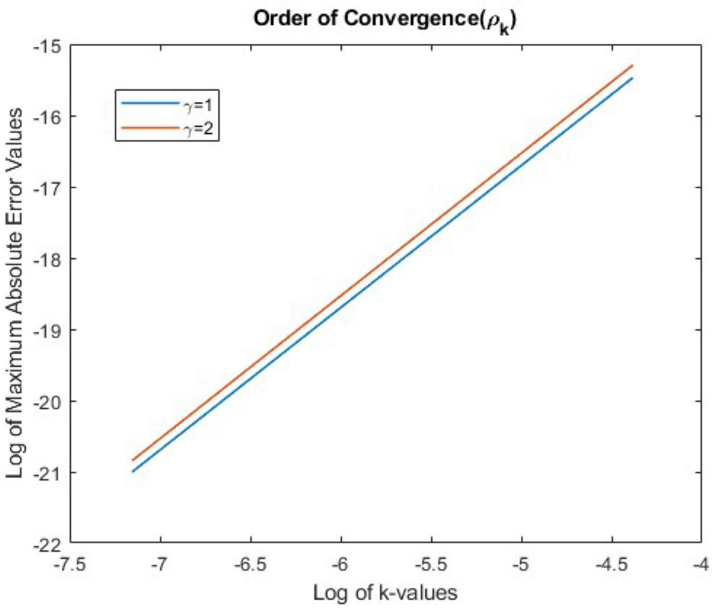

(d): log-log error plot with $\gamma = 1, 2$ for Example 1

Fig. 1 continued

where $e_{h_{x_1}}$ and $e_{h_{x_2}}$ are the maximum absolute errors for spatial uniform mesh sizes h_{x_1} and h_{x_2}, respectively, and the temporal rate of convergence ρ_k is computed by:

$$\rho_k = \frac{\log(e_{k_1}/e_{k_2})}{\log(k_1/k_2)}, \tag{5.2}$$

where e_{k_1} and e_{k_2} are the maximum absolute errors for temporal grid sizes k_1 and k_2, respectively.

Example 1 Heat equation in polar cylindrical coordinates

$$\frac{\partial^2 u}{\partial r^2} + \frac{\gamma}{r}\frac{\partial u}{\partial r} + \frac{\partial^2 u}{\partial z^2} = \frac{\partial u}{\partial t} + G(r, z, t), \tag{5.3}$$

where $0 < r, z < 1, t > 0$. The analytical solution is $u(r, z, t) = e^{-\gamma t} \cosh r \cosh z$. Table 1 contains a tabulation of the MAEs taken at time $t = 1$ for $\gamma = 1, 2$ and with a constant value of mesh ratio parameter $\lambda = 3.2$. In this table, we have compared our results with those obtained by the method discussed in [35]. For a fixed value of the parameter $\lambda = 3.2$, $\gamma = 2$, the spatial and temporal order of convergence ρ_h and ρ_k are also calculated using the formulas (5.1) and (5.2), respectively. The proposed method (4.9)-(4.10) gives the required accuracy as shown by the computed order in this table for various values of γ.

In Fig. 1(a)-(b), we provide the three-dimensional visualisations of numerical and analytical solutions for $\gamma = 1$, step size $h = \frac{1}{16}$, $\lambda = 3.2$ at $t = 1$. These figures exhibit that the numerical and analytical solutions are well consistent in three-dimensional form. The log-log errors are graphed in Fig. 1(c) and (d) for $\gamma = 1$ and 2 showing the order of convergence ρ_h and ρ_k. It is evident from these figures that the slope of the lines in Fig. 1(c) is approximately four and in Fig. 1(d) is approximately two.

Example 2 Quasi-linear Problem

$$\left(1 + u^2 + e^t \cos x \sin y\right) u_{xx} + \left(1 + u^2 + e^t \sin x \cos y\right) u_{yy} = u_t + \alpha u\,(u_x + u_y) + f(x, y, t), \tag{5.4}$$

where $0 < x, y < 1, t > 0$. There is a analytical solution supplied by $u = e^t \cos x \cos y$. Table 2 lists the MAEs at time $t = 1$ for the value of $\alpha = 1, 10, 25$, and a fixed $\lambda = 3.2$. The results we obtained have been juxtaposed with the findings obtained by the method discussed in [35]. The order of convergence ρ_h and ρ_k are also calculated using the formula (5.1) and (5.2) in this table. The fourth-order convergence of the suggested method is endorsed by the computational results in this table. In this table, the number of iterations are also mentioned for each step size and $\alpha = 1, 10, 25$. Here, CPU time is also given (in seconds) to show the efficiency of the proposed method.

Table 2 MAEs at $t = 1$ for Example 2

h	Proposed Scheme (2.57)						Method discussed in [35]		
	$\alpha = 1$	Itr.	$\alpha = 10$	Itr.	$\alpha = 25$	Itr.	$\alpha = 1$	$\alpha = 10$	$\alpha = 25$
1/8	9.5450e−06	60	6.3480e−06	59	3.2710e−05	58	4.9045e−05	2.2998e−05	3.8014e−04
CPU Time	(0.1087)		(0.1631)		(0.0940)		(0.1141)	(0.1712)	(0.1801)
ρ_h	3.9989		3.9495		3.9950		3.9995	3.9997	3.9961
ρ_k	1.9995		1.9748		1.9975		1.9997	1.9998	1.9981
1/16	5.9700e−07	84	4.1088e−07	84	2.0515e−06	87	3.0664e−06	1.4377e−06	2.3823e−05
CPU Time	(0.8767)		(0.9113)		(0.8753)		(0.8823)	(0.9568)	(0.9607)
ρ_h	3.9903		3.9992		3.9968		3.9999	4.0000	3.9996
ρ_k	1.9952		1.9996		1.9984		2.0000	2.0000	1.9998
1/32	3.7563e−08	88	2.5694e−08	89	1.2850e−07	96	1.9166e−07	8.9856e−08	1.4893e−06
CPU Time	(8.8721)		(9.4554)		(9.8926)		(9.3157)	(9.9252)	(10.3872)
ρ_h	4.0001		4.0000		3.9975		4.0039	4.0035	4.0000
ρ_k	2.0000		2.0000		1.9988		2.0020	2.0017	2.0000
1/64	2.3476e−09	80	1.6059e−09	80	8.0450e−09	89	1.1946e−08	5.6024e−09	9.3084e−08
CPU Time	(126.1270)		(135.9091)		(143.9331)		(132.3169)	(142.7044)	(148.1296)

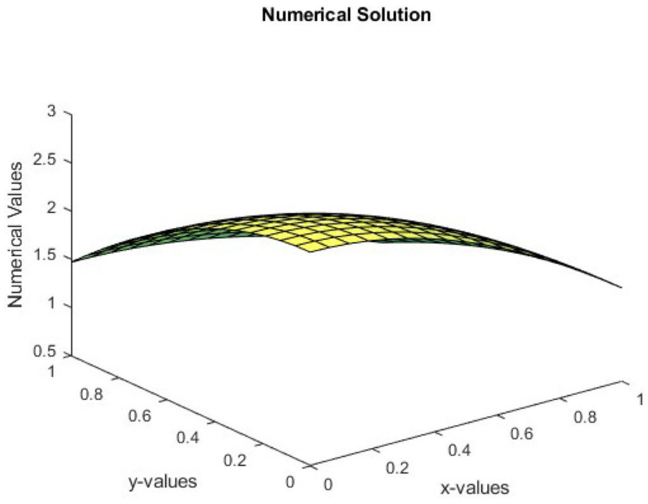

(a): Numerical Solutions with $h = \frac{1}{16}, \alpha = 10$ at $t = 1$ for Example 2

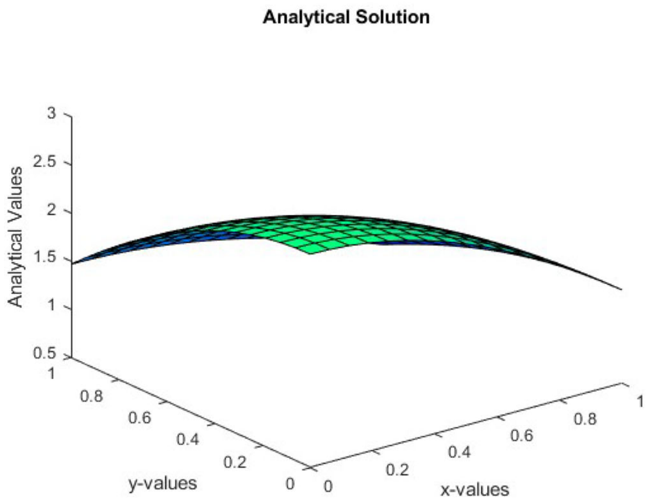

(b): Analytical Solutions with $h = \frac{1}{16}, \alpha = 10$ at $t = 1$ for Example 2

Fig. 2 (a) Numerical Solutions with $h = \frac{1}{16}, \alpha = 10$ at $t = 1$ for Example 2. (b) Analytical Solutions with $h = \frac{1}{16}, \alpha = 10$ at $t = 1$ for Example 2. (c) log-log error plot with $\alpha = 1, 10, 25$ for Example 2. (d) log-log error plot with $\alpha = 1, 10, 25$ for Example 2

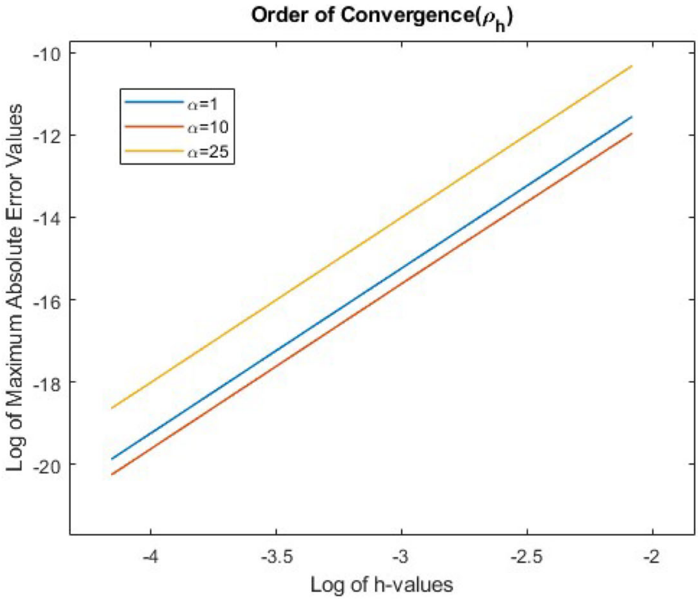

Fig. 2(c): log-log error plot with $\alpha = 1, 10, 25$ for Example 2

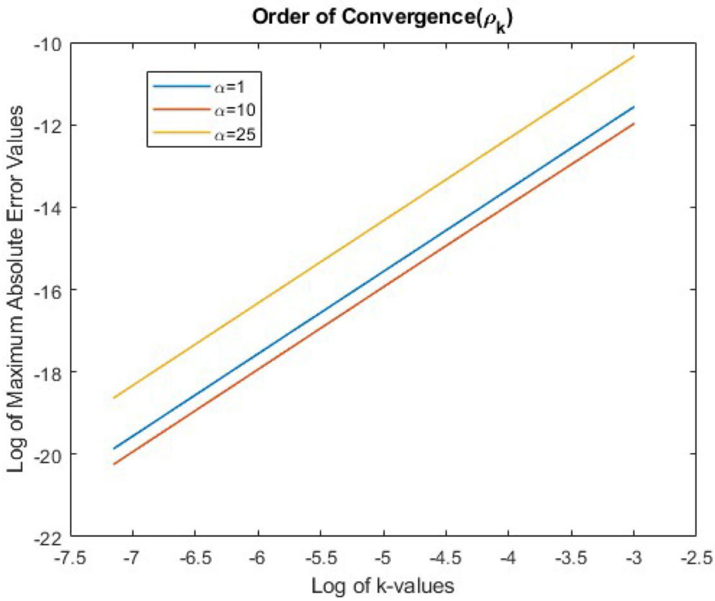

Fig. 2(d): log-log error plot with $\alpha = 1, 10, 25$ for Example 2

Fig. 2 continued

Table 3 MAEs at $t = 1$ for Example 3

h	Proposed Scheme (2.57)			Method discussed in [36]		
	$\epsilon = 10^{-2}$	$\epsilon = 10^{-4}$	$\epsilon = 10^{-6}$	$\epsilon = 10^{-2}$	$\epsilon = 10^{-4}$	$\epsilon = 10^{-6}$
1/20	2.9561e−07	1.7065e−10	1.7860e−14	1.2577e−06	1.2198e−09	1.4275e−13
CPU Time(s)	(0.2004)	(0.1819)	(0.0936)	(0.2104)	(0.1909)	(0.1012)
ρ_h	3.9984	3.9994	3.9988	4.0155	3.9797	3.9914
ρ_k	1.9992	1.9997	1.9994	2.0077	1.9899	1.9957
1/40	1.8496e−08	1.0670e−11	1.1172e−15	7.7768e−08	7.7317e−11	8.9754e−15
CPU Time(s)	(1.1202)	(0.7405)	(0.4076)	(1.1762)	(0.7776)	(0.4279)
ρ_h	3.9959	4.0065	4.0081	4.0206	4.0066	4.0045
ρ_k	1.9979	2.0032	2.0040	2.0103	2.0033	2.0022
1/80	1.1593e−09	6.6390e−13	6.9436e−17	4.7916e−09	4.8101e−12	5.5923e−16
CPU Time(s)	(14.4914)	(10.1451)	(8.0054)	(15.2158)	(10.6522)	(8.4056)

Figure 2(a) and (b) show 3D graphs of numerical solutions and the analytical solutions, respectively, with $h = 1/16$, $\alpha = 10$ and $\lambda = 3.2$ at time $t = 1$. These figures demonstrate good consistency between the analytical and numerical solutions in three dimensions. In Fig. 2(c), the log-log errors are displayed for $\alpha = 1, 10$ and 25 showing the order of convergence ρ_h, and for the order of convergence ρ_k, the Fig. 2(d) is presented. We can say from these figures that the slope of the lines in Fig. 2(c) is approximately four and in Fig. 2(d) is approximately two.

Example 3 Viscous unsteady Burgers' equation
Consider the unsteady viscous Burgers' equation:

$$\epsilon(u_{xx} + u_{yy}) = u_t + u(u_x + u_y), \quad 0 < x, y < 1, \ t > 0 \tag{5.5}$$

The analytical solution is presented by [54]:

$$u(x, y, t) = \frac{2\epsilon\pi \sin[\pi(x + y)]\, e^{-2\epsilon\pi^2 t}}{2 + \cos[\pi(x + y)]\, e^{-2\epsilon\pi^2 t}}$$

The MAEs for u are listed in Table 3 at $t = 1$ for the values of $\epsilon = 10^{-2}, 10^{-4}, 10^{-6}$. The current outcomes are contrasted to those obtained using the approach given in [36]. For a fixed value of $\lambda = 1.6$, the proposed method (2.57) behaves like a fourth order method for various values of ϵ which has been verified by calculating the order of convergence ρ_h using the formula (5.1). In this table, we have discussed the order of convergence ρ_h and ρ_k for $\epsilon = 10^{-2}, 10^{-4}, 10^{-6}$. Also, we have shown the computational time (in seconds) for these values of ϵ to verify the efficiency of the proposed method.

Figure 3(a)-(b) depict the numerical solution derived by the suggested approach and the actual solution of the above equation (5.5) for $h = 1/40$, $\lambda = 1.6$ and $\epsilon = 10^{-4}$ at $t = 1$. These figures show that both the numerical and analytical solutions exhibit high consistency in their three-dimensional representations. Figure 3(c) shows a graph of log-log errors for the values of $\epsilon = 10^{-2}, 10^{-4}$ and 10^{-6}. This figure clearly illustrates the graph's approximately four-degree slope which shows the required the order of convergence ρ_h.

Example 4 Time-dependent NSEs of Motion
Consider the following time-dependent incompressible NSEs of motion:

$$\epsilon(u_{xx} + u_{yy}) = u_t + uu_x + vu_y + p_x, \tag{5.6}$$

$$\epsilon(v_{xx} + v_{yy}) = v_t + uv_x + vv_y + p_y, \tag{5.7}$$

where $0 < x, y < \pi$, $t > 0$, Reynolds number $R = \frac{1}{\epsilon}$.

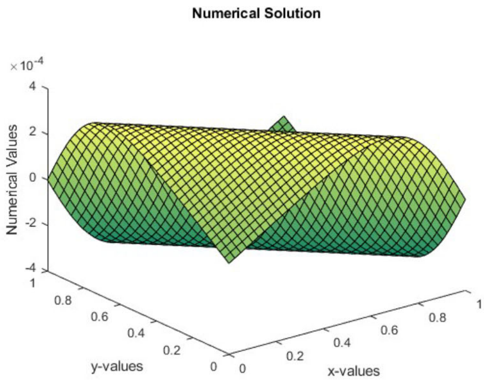

(a): Numerical Solutions with $h = \frac{1}{40}, \epsilon = 10^{-4}$ at $t = 1$ for Example 3

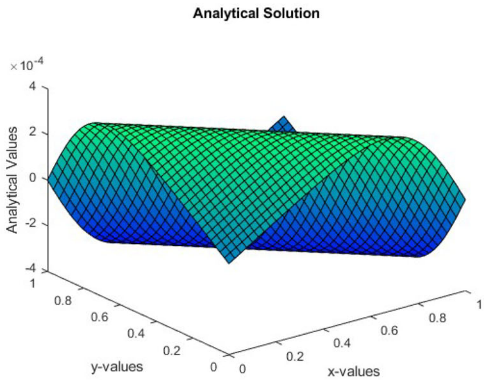

(b): Analytical Solutions with $h = \frac{1}{40}, \epsilon = 10^{-4}$ at $t = 1$ for Example 3

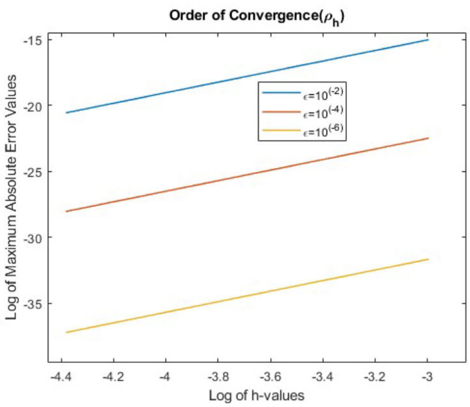

(c): log-log error plot with $\epsilon = 10^{-2}, 10^{-4}, 10^{-6}$ for Example 3

Fig. 3 (a) Numerical Solutions with $h = \frac{1}{40}$, $\epsilon = 10^{-4}$ at $t = 1$ for Example 3. (b) Analytical Solutions with $h = \frac{1}{40}$, $\epsilon = 10^{-4}$ at $t = 1$ for Example 3. (c) log-log error plot with $\epsilon = 10^{-2}$, 10^{-4}, 10^{-6} for Example 3

The analytical solutions are provided by [6]:

$$u = -e^{-2\epsilon t} \cos x \sin y \text{ and } v = e^{-2\epsilon t} \sin x \cos y$$

and the pressure function is given as:

$$p(x, y, t) = -\frac{e^{-4\epsilon t}(\cos 2x + \cos 2y)}{4}.$$

In Table 4, we have shown the maximum absolute errors for the variables u and v that are calculated at time $t = 1$ for the fixed value of $\lambda = 1.6/\pi^2$. Clearly, the results that we obtained for the equation (5.6)-(5.7) have been juxtaposed with those obtained by the approach in [36] for the values of $\epsilon = 0.1, 0.02$. In this table, the number of iterations are also mentioned for each step size and $\epsilon = 0.1, 0.02$. Here, CPU time (in seconds) is also given to show the efficiency of the proposed method.

Figure 4(a)-(d) are the plots of numerical and analytical solutions of u and v with the step size $h = \pi/40$, $\lambda = 1.6/\pi^2$ and $\epsilon = 0.1$ at $t = 1$. The log-log errors are also graphed in Fig. 4(e)-(f) with $\epsilon = 0.1$ and 0.02 for both the variables u and v. From these figures, one can easily calculate the slope of the graphs that is almost four, i.e. the order of convergence ρ_h for both the variables u and v is approximately four.

Example 5 Taylor-Vortex Problem

Here, we figure out the system (5.6)-(5.7) with the pressure function given as:

$$p(x, y, t) = -\frac{e^{-4\epsilon N^2 t}\left(\cos\left(2Nx\right) + \cos\left(2Ny\right)\right)}{4},$$

Table 4 MAEs at $t = 1$ for Example 4

h		Proposed Scheme (3.27)				Method discussed in [36]	
		$\epsilon = 0.1$	Itr.	$\epsilon = 0.02$	Itr.	$\epsilon = 0.1$	$\epsilon = 0.02$
$\frac{\pi}{20}$	u	1.4024e−05	13	1.4770e−04	41	6.1385e−05	6.7879e−04
	v	2.2624e−05		3.2949e−04		7.7378e−05	8.1354e−04
CPU Time(s)		(0.3958)		(0.9547)		(0.4155)	(0.9899)
$\frac{\pi}{40}$	u	8.6564e−07	11	9.2114e−06	22	3.8617e−06	4.2670e−05
	v	1.4204e−06		2.0307e−05		4.8960e−06	5.1596e−05
CPU Time(s)		(2.5237)		(4.1389)		(2.6498)	(4.2458)
$\frac{\pi}{80}$	u	5.3686e−08	9	5.7418e−07	13	2.4172e−07	2.6706e−06
	v	8.7973e−08		1.2592e−06		3.0697e−07	3.2309e−06
CPU Time(s)		(27.0174)		(39.7328)		(28.3683)	(41.1183)
$\frac{\pi}{160}$	u	3.3483e−09	7	3.5874e−08	10	1.5114e−08	1.6696e−07
	v	5.4893e−09		7.8305e−08		1.9133e−08	2.0184e−07
CPU Time(s)		(950.651)		(1121.218)		(982.535)	(1162.316)

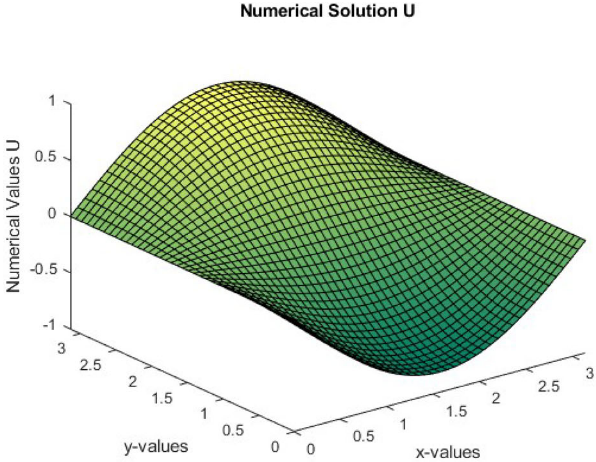

(a): Numerical Solutions of u with $h = \frac{\pi}{40}, \epsilon = 0.1$ at $t = 1$ for Example 4

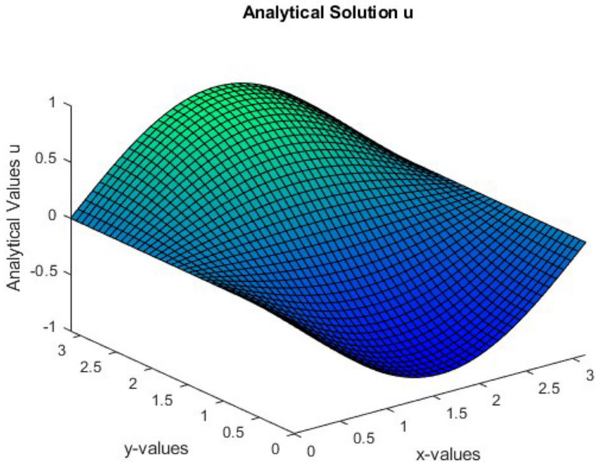

(b): Analytical Solutions of u with $h = \frac{\pi}{40}, \epsilon = 0.1$ at $t = 1$ for Example 4

Fig. 4 (a) Numerical Solutions of u with $h = \frac{\pi}{40}, \epsilon = 0.1$ at $t = 1$ for Example 4. (b) Analytical Solutions of u with $h = \frac{\pi}{40}, \epsilon = 0.1$ at $t = 1$ for Example 4. (c) Numerical Solutions of v with $h = \frac{\pi}{40}, \epsilon = 0.1$ at $t = 1$ for Example 4. (d) Analytical Solutions of v with $h = \frac{\pi}{40}, \epsilon = 0.1$ at $t = 1$ for Example 4. (e) log-log error plot for u with $\epsilon = 0.1, 0.02$ for Example 4. (f) log-log error plot for v with $\epsilon = 0.1, 0.02$ for Example 4

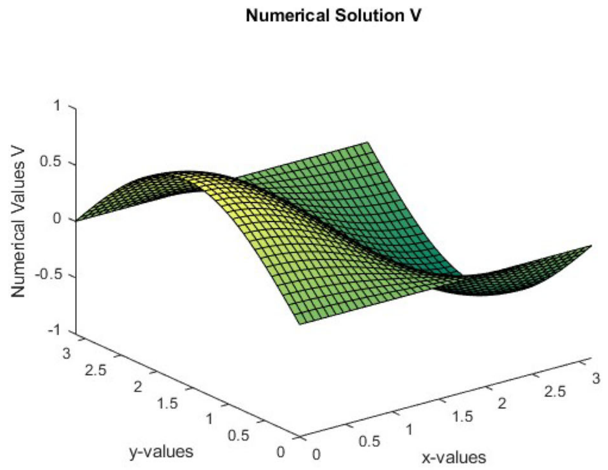

(c): Numerical Solutions of v with $h = \frac{\pi}{40}, \epsilon = 0.1$ at $t = 1$ for Example 4

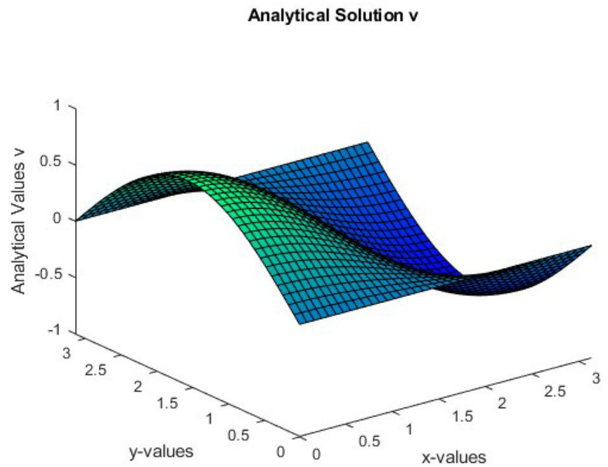

(d): Analytical Solutions of v with $h = \frac{\pi}{40}, \epsilon = 0.1$ at $t = 1$ for Example 4

Fig. 4 continued

where N is the total quantity of the vortices. The analytical solutions are provided by: $u = -e^{-2\epsilon N^2 t} \cos(Nx) \sin(Ny)$ and $v = e^{-2\epsilon N^2 t} \sin(Nx) \cos(Ny)$.

Table 5 lists the MAEs for the variables u and v at the time $t = 1$ for $N = 4$, $\lambda = 1.6/\pi^2$ and step-sizes $h = \pi/20, \pi/40, \pi/80$ and $\pi/160$. The results of our study and those obtained by the technique used in [35] have been compared in this table for the value of $\epsilon = 0.1$ and 0.02 and different spatial step-sizes.

The numerical and analytical solutions for the problem Example 5 are plotted in Fig. 5(a)-(d) for unknowns u and v with the step size $h = \pi/40$, $\lambda = 1.6/\pi^2$, $N = 4$

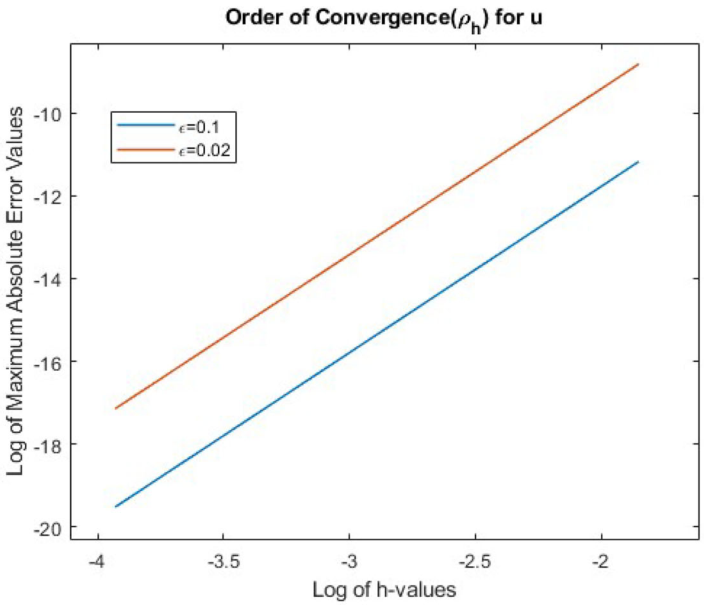

(e): log-log error plot for u with $\epsilon = 0.1, 0.02$ for Example 4

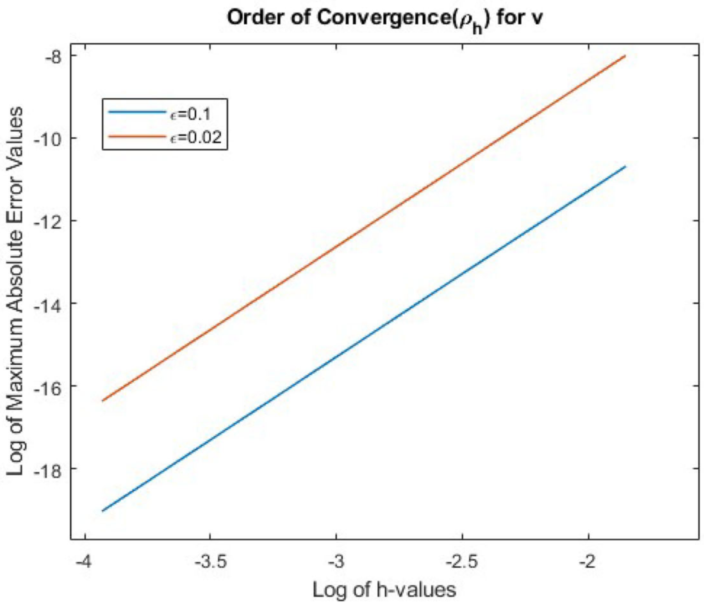

(f): log-log error plot for v with $\epsilon = 0.1, 0.02$ for Example 4

Fig. 4 continued

Table 5 MAEs at $t = 1$ for Example 5

h		Proposed Scheme (3.27)		Method discussed in [35]	
		$\epsilon = 0.1$	$\epsilon = 0.02$	$\epsilon = 0.1$	$\epsilon = 0.02$
$\frac{\pi}{20}$	u	2.1027e−05	2.6629e−04	3.9424e−05	4.2244e−04
	v	2.1027e−05	2.6629e−04	3.9424e−05	4.2244e−04
$\frac{\pi}{40}$	u	1.0689e−06	1.5119e−05	2.5936e−06	3.5795e−05
	v	1.0689e−06	1.5119e−05	2.5936e−06	3.5795e−05
$\frac{\pi}{80}$	u	6.3116e−08	8.9191e−07	1.6315e−07	2.3277e−06
	v	6.3116e−08	8.9191e−07	1.6315e−07	2.3277e−06
$\frac{\pi}{160}$	u	3.8780e−09	5.4494e−08	1.0065e−08	1.4205e−07
	v	3.8780e−09	5.4494e−08	1.0065e−08	1.4205e−07

and the viscosity coefficient $\epsilon = 0.02$ at the time $t = 1$. The log-log errors are also portrayed in Fig. 5(e) with $\epsilon = 0.1$ and 0.02 for the variables u and v. This plot indicates that the graph's slope is nearly four which verifies the required accuracy.

Example 6 EFK Equation

Consider the following two-dimensional EFK equation:

$$u_t + \gamma \nabla^4 u - \nabla^2 u + g(u) = 0, \quad (x, y, t) \in \Omega, \tag{5.8}$$

where $\Omega = \{(x, y, t) : 0 < x, y < 1, t > 0\}$ and $g(u) = u^3 - u$. Here, γ is a positive real number and the initial condition is given by:

$$u(x, y, 0) = x^3 y^3 (1 - x)^3 (1 - y)^3, \quad 0 < x, y < 1 \tag{5.9}$$

and boundary conditions are:

$$u = 0, \ \nabla^2 u = 0, \quad (x, y, t) \in \partial\Omega \times (0, T], \tag{5.10}$$

T being the final computational time. The numerical solution of (5.8) subject to (5.9)-(5.10) corresponding to $\gamma = 0.1$ at $t = 1$ obtained using the proposed method (3.30)-(3.31) is displayed in Fig. 6 with $k = h = 0.025$. Identical features to those described in [20] and [26] may be seen in the solution profile.

Example 7 Non-homogeneous EFK Equation

Take into consideration the non-homogeneous EFK equation shown below:

$$u_t + \gamma \nabla^4 u - \nabla^2 u + g(u) = s(x, y, t), \quad (x, y) \in \Omega, t > 0 \tag{5.11}$$

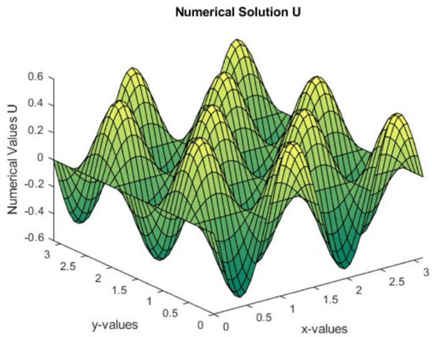

(a): Numerical Solutions of u with $h = \frac{\pi}{40}, N = 4, \epsilon = 0.02$ at $t = 1$ for Example 5

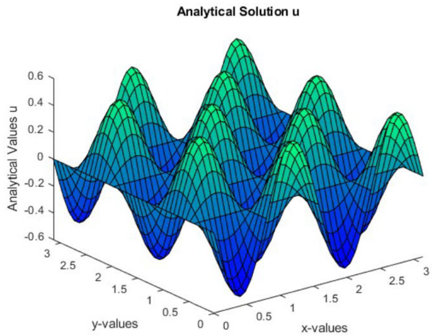

(b): Analytical Solutions of u with $h = \frac{\pi}{40}, N = 4, \epsilon = 0.02$ at $t = 1$ for Example 5

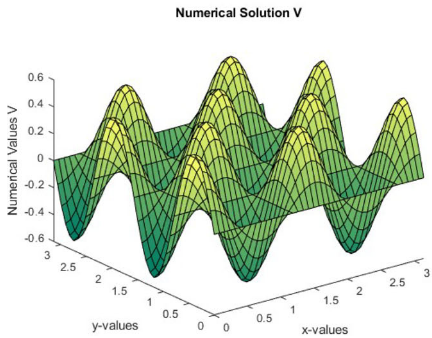

(c): Numerical Solutions of v with $h = \frac{\pi}{40}, N = 4, \epsilon = 0.02$ at $t = 1$ for Example 5

Fig. 5 (a) Numerical Solutions of u with $h = \frac{\pi}{40}$, $N = 4$, $\epsilon = 0.02$ at $t = 1$ for Example 5. (b) Analytical Solutions of u with $h = \frac{\pi}{40}$, $N = 4$, $\epsilon = 0.02$ at $t = 1$ for Example 5. (c) Numerical Solutions of v with $h = \frac{\pi}{40}$, $N = 4$, $\epsilon = 0.02$ at $t = 1$ for Example 5. (d) Analytical Solutions of v with $h = \frac{\pi}{40}$, $N = 4$, $\epsilon = 0.02$ at $t = 1$ for Example 5. (e) log-log error plot for u and v with $\epsilon = 0.1, 0.02$ for Example 5

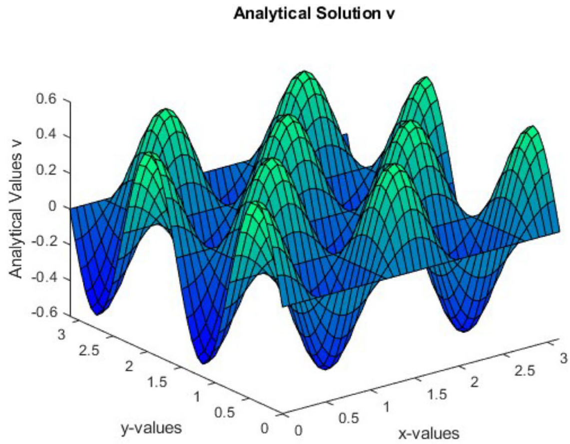

(d): Analytical Solutions of v with $h = \frac{\pi}{40}, N = 4, \epsilon = 0.02$ at $t = 1$ for Example 5

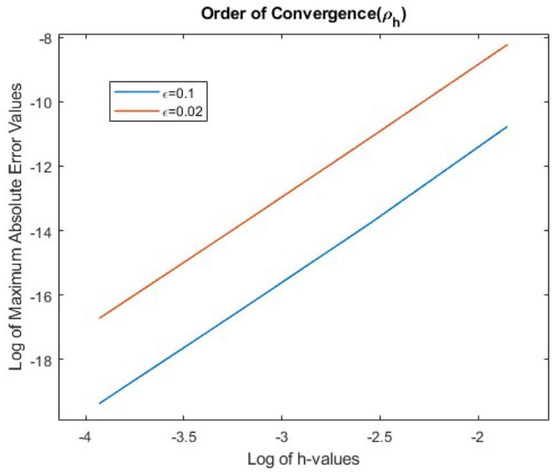

(e): log-log error plot for u and v with $\epsilon = 0.1, 0.02$ for Example 5

Fig. 5 continued

where $\Omega = (0, 1) \times (0, 1)$, $g(u) = u^3 - u$ and the analytical solution is given by [26]:

$$u(x, y, t) = e^{-t} \sin(2\pi x) \sin(2\pi y). \tag{5.12}$$

Using equation (5.12) and setting $t = 0$ yields the initial condition, and this problem is evaluated with respect to the following boundary conditions:

$$u = 0, \;\; \nabla^2 u = 0, \quad (x, y) \in \partial\Omega, t > 0.$$

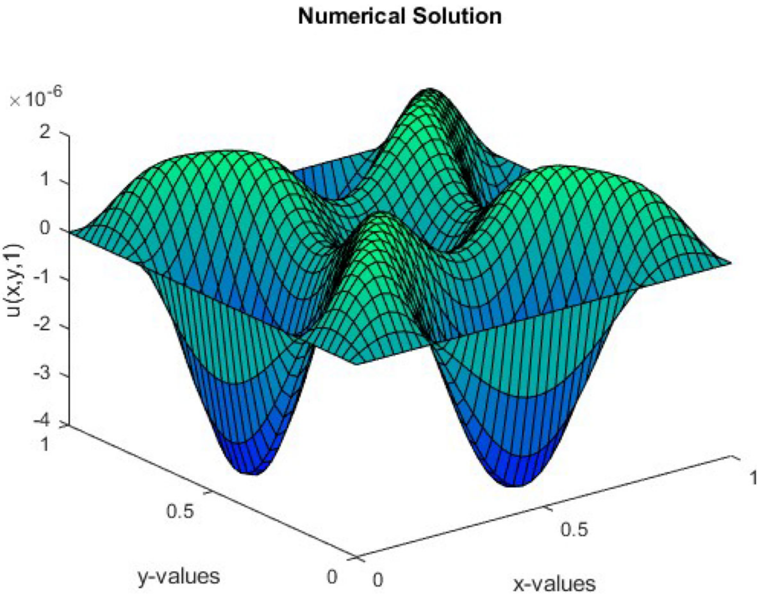

Fig. 6 Numerical Solutions with $h = k = 0.025$, $\gamma = 0.1$ at $t = 1$ for Example 6

The analytical solution (5.12) is used to derive the right hand side function $s(x, y, t)$ as a test method. We use the suggested difference technique (3.30)-(3.31) to solve the equation (5.12). We have discussed the MAEs at the final time $t = 1$ in Table 6 with $\gamma = 0.01$, taking into account $k = h$ for each mesh. We have compared our results with those obtained in [20] and [26] in this table. In Table 7, the maximum absolute errors are presented with the mesh ratio parameter set at $\lambda = 1.6$ at time $t = 0.25$ seconds for both the variables u and $\nabla^2 u$. The proposed method (3.30)-(3.31) provides convergence to a fourth order as shown by the numerical data ρ_h in this table calculated by the formula (5.1).

Moreover, the plot of numerical and analytical results for $\gamma = 0.01$ at time $t = 1$ with step-size $h = k = 0.025$ are depicted in Fig. 7(a)-(b). These figures exhibit that the numerical and analytical solutions are well consistent in three-dimensional form. The log-log errors are graphed in Fig. 7(c) and (d) with $\gamma = 0.2, 0.02$ and 0.002 showing the order of convergence ρ_h and ρ_k for u.

Example 8 Non-homogeneous KS Equation

Take into account the space derivative version of the non-homogeneous two-dimensional KS equation [27]:

$$u_t + \nabla^4 u + \nabla^2 u + u(u_x + u_y) = s(x, y, t), \quad (x, y) \in \Omega, t > 0 \tag{5.13}$$

where $\Omega = (-1, 1) \times (-1, 1)$ and the analytical solution is given by [55]:

$$u(x, y, t) = e^{-t} \cos(\pi x) \cos(\pi y).$$

Table 6 MAEs at $t = 1$ with $\gamma = 0.01$ for Example 7

$h = k$	Proposed Scheme (3.30)-(3.31)	Khiari and Omrani [26]	Ilati and Dehghan [20]
$\frac{1}{10}$	5.5030e−04	–	6.0212e−03
$\frac{1}{15}$	2.4894e−04	0.0064	–
$\frac{1}{20}$	1.2984e−04	0.0038	1.3589e−03
$\frac{1}{25}$	7.9560e−05	0.0022	–
$\frac{1}{30}$	5.3588e−05	0.0016	–
$\frac{1}{40}$	2.9780e−05	8.1310e−04	2.3295e−04
$\frac{1}{50}$	1.8778e−05	4.4541e−04	–

Table 7 MAEs at $t = 0.25$ with $\lambda = 1.6$ and Order of Convergence ρ_h for Example 7

h	Solution Variables	$\gamma = 0.2$		$\gamma = 0.02$		$\gamma = 0.002$	
		MAE	ρ_h	MAE	ρ_h	MAE	ρ_h
$\frac{1}{8}$	u	1.5928e−03	–	1.3379e−03	–	9.6605e−04	–
	$\nabla^2 u$	1.4325e−01	–	1.2336e−01	–	9.3733e−02	–
$\frac{1}{16}$	u	1.0276e−04	3.9542	8.6349e−05	3.9536	6.2289e−05	3.9550
	$\nabla^2 u$	9.2559e−03	3.9520	7.9556e−03	3.9548	6.0410e−03	3.9557
$\frac{1}{32}$	u	6.4672e−06	3.9900	5.4343e−06	3.9900	3.9196e−06	3.9902
	$\nabla^2 u$	5.8254e−04	3.9899	5.0066e−04	3.9901	3.8014e−04	3.9902

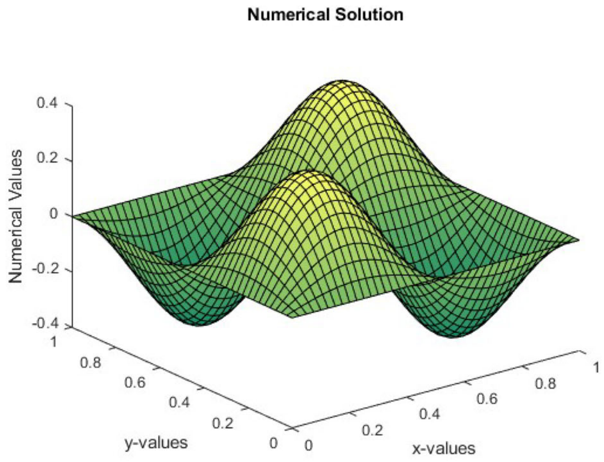

(a): Numerical Solutions with $h = k = \frac{1}{40}, \gamma = 0.01$ at $t = 1$ for Example 7

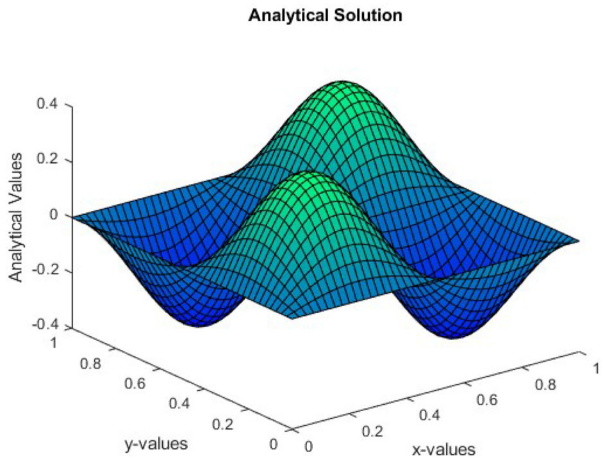

(b): Analytical Solutions with $h = k = \frac{1}{40}, \gamma = 0.01$ at $t = 1$ for Example 7

Fig. 7 (a) Numerical Solutions with $h = k = \frac{1}{40}$, $\gamma = 0.01$ at $t = 1$ for Example 7. (b) Analytical Solutions with $h = k = \frac{1}{40}$, $\gamma = 0.01$ at $t = 1$ for Example 7. (c) log-log error plot with $\gamma = 0.2, 0.02, 0.002$ for Example 7. (d) log-log error plot with $\gamma = 0.2, 0.02, 0.002$ for Example 7

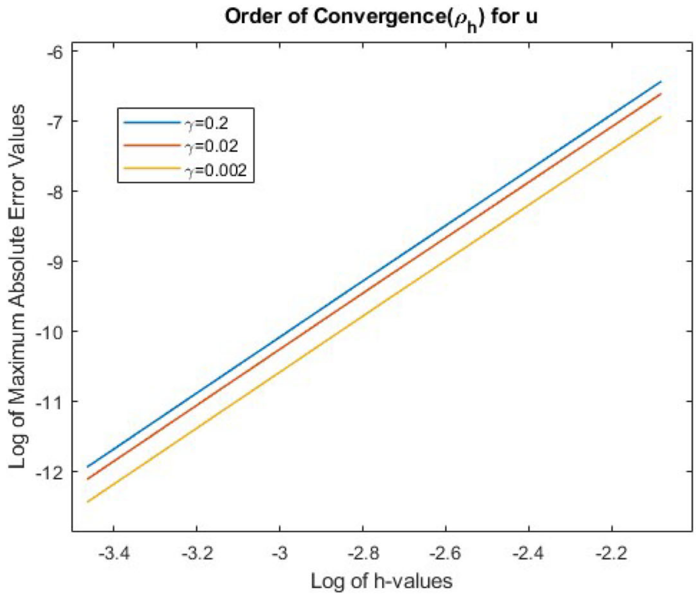

(c): log-log error plot with $\gamma = 0.2, 0.02, 0.002$ for Example 7

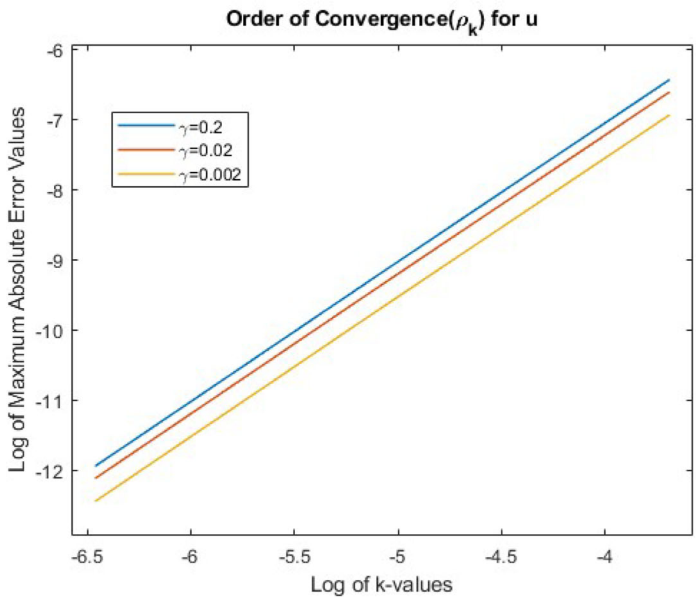

(d): log-log error plot with $\gamma = 0.2, 0.02, 0.002$ for Example 7

Fig. 7 continued

Table 8 MAEs at $t = 1$ and Order of Convergence for Example 8

h	Solution Variables	Proposed Scheme (3.30)-(3.31)		
		MAEs	ρ_h	ρ_k
$\frac{1}{4}$	u	4.3444e−03	–	–
	$\nabla^2 u$	7.4154e−02	–	–
CPU Time(s)		(0.0599)		
$\frac{1}{8}$	u	2.7351e−04	3.9895	1.9947
	$\nabla^2 u$	4.7012e−03	3.9794	1.9897
CPU Time(s)		(0.4652)		
$\frac{1}{16}$	u	1.7106e−05	3.9990	1.9995
	$\nabla^2 u$	2.9478e−04	3.9953	1.9977
CPU Time(s)		(14.1229)		

In Table 8, we have presented the MAEs for $\lambda = 1.6$ with distinct grid spacing to represent the order of magnitude of discussed scheme (3.30)-(3.31) at time $t = 1$. The proposed method (3.30)-(3.31) show the fourth order accuracy for both u and $\nabla^2 u$. We have discussed the computational time in seconds here. In this table, we have also calculated the order of convergence ρ_h and ρ_k using the formulas (5.1) and (5.2).

Figure 8(a)-(b) present the numerical and analytical solutions for $h = 1/16$, $\lambda = 1.6$ at time $t = 1$. These figures exhibit that the numerical and analytical solutions are well consistent in three-dimensional form. The Fig. 8(c) represents the log-log errors for u. We have displayed the order of convergence ρ_h and ρ_k in this figure to verify the required accuracy.

6 Concluding remarks

We have provided a computational technique in exponential form for investigating numerical solutions of the 2D quasi-linear parabolic PDEs. The proposed two-level implicit difference technique is second-order accurate in time and fourth-order accurate in space. We have developed the corresponding ADI scheme for the linear parabolic PDE of order two, which is demonstrated to be unconditionally stable. Further, the two-level method has been applied to the fourth-order parabolic PDEs without the use of any additional nodes or special schemes near the boundary of the solution domain. The proposed scheme has been successfully experimented on quasi-linear second- and fourth-order 2D parabolic PDEs (5.3)-(5.13), and the results provided in this study have achieved high-order accurate results. The advantage of the present study is that it gives better results than the existing fourth-order accurate methods in the literature. Based on the outcomes, we can extend our approach to the three-dimensional parabolic PDEs in the future. Also, we can try to solve the higher-dimensional parabolic PDEs in different types of domains.

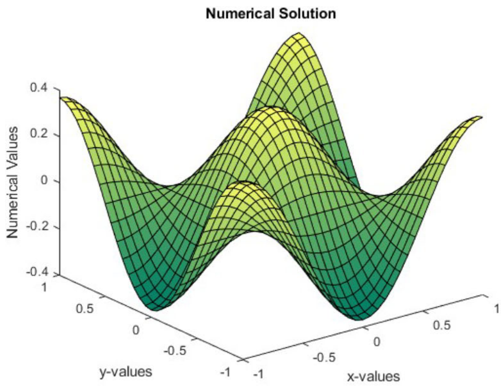

(a): Numerical Solutions with $h = \frac{1}{16}$ at $t = 1$ for Example 8

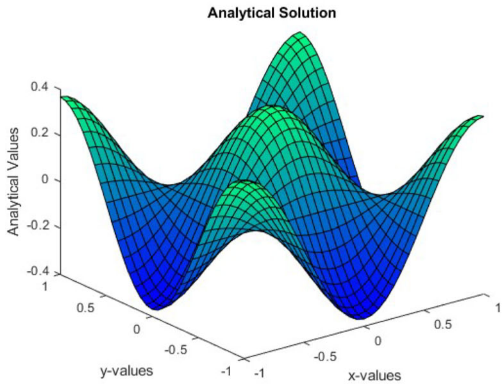

(b): Analytical Solutions with $h = \frac{1}{16}$ at $t = 1$ for Example 8

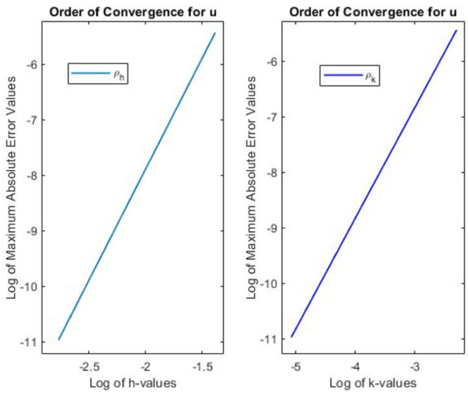

(c): log-log error plot for Example 8

Fig. 8 (a) Numerical Solutions with $h = \frac{1}{16}$ at $t = 1$ for Example 8. (b) Analytical Solutions with $h = \frac{1}{16}$ at $t = 1$ for Example 8. (c) log-log error plot for Example 8

Acknowledgements The authors thank the reviewers for their valuable suggestions, which substantially improved the standard of the paper.

Author Contributions Divya Sharma, Kajal Mittal, and Deepti Kaur wrote the main manuscript. Rajendra K. Ray and R.K. Mohanty reviewed the manuscript.

Funding This work is partly supported by the University Grant Commission (UGC), New Delhi, India, Ref. No. 1087/(CSIR-UGC NET DEC. 2016) and 1058/(CSIR-UGC NET DEC. 2018) to the first and second authors, respectively. The third author received partial support from the Science and Engineering Research Board (SERB), Department of Science & Technology (DST), Government of India, Sanction Order No.: CRG/2018/004608.

Data Availability No datasets were generated or analysed during the current study.

Declarations

Competing interests The authors declare no competing interests.

Ethical approval This article does not contain any study with human participants or animals performed by any of the authors.

References

1. Abbaszadeh, M., Dehghan, M.: Reduced order modeling of time-dependent incompressible Navier-Stokes equation with variable density based on a local radial basis functions-finite difference (LRBF-FD) technique and the POD/DEIM method. Comput. Methods Appl. Mech. Eng. **364**, 112914 (2020). https://doi.org/10.1016/j.cma.2020.112914
2. Aggul, M., Labovsky, A.: A high accuracy minimally invasive regularization technique for Navier-Stokes equations at high Reynolds number. Numer. Methods Partial Differ. Equations **33**(3), 814–839 (2017). https://doi.org/10.1002/num.22124
3. Aronson, D.G., Weinberger, H.F.: Multidimensional nonlinear diffusion arising in population genetics. Adv. Math. **30**, 33–76 (1978). https://doi.org/10.1016/0001-8708(78)90130-5
4. Bai, Z.Z., Ran, Y.H., Yuan, L.: On approximated ILU and UGS preconditioning methods for linearized discretized steady incompressible Navier-Stokes equations. Numer. Algorithms **65**, 43–68 (2014). https://doi.org/10.1007/s11075-013-9694-y
5. Balzano, A.: MOSQUITO: An efficient finite difference scheme for numerical simulation of 2D advection. Int. J. Numer. Methods Fluids **31**(2), 481–496 (1999). https://doi.org/10.1002/(SICI)1097-0363(19990930)31:2<481::AID-FLD886>3.0.CO;2-I
6. Chorin, A.J.: Numerical solution of the Navier-Stokes equations. Math. Comp. **22**, 745–762 (1968). https://doi.org/10.1090/S0025-5718-1968-0242392-2
7. Dai, W., Nassar, R.: Compact ADI method for solving parabolic differential equations. Numer. Methods Partial Differ. Equations **18**(2), 129–142 (2002). https://doi.org/10.1002/num.1037
8. Danumjaya, P., Pani, A.K.: Orthogonal cubic spline collocation method for the extended Fisher-Kolmogorov equation. J. Comput. Appl. Math. **174**, 101–117 (2005). https://doi.org/10.1016/j.cam.2004.04.002
9. Dee, G.T., Saarloos, W.V.: Bistable systems with propagating fronts leading to pattern formation. Phys. Rev. Lett. **60**, 2641–2644 (1988). https://doi.org/10.1103/PhysRevLett.60.2641
10. Dehghan, M., Mohammadi, V.: Two-dimensional simulation of the damped Kuramoto-Sivashinsky equation via radial basis function-generated finite difference scheme combined with an exponential time discretization. Eng. Anal. Bound. Elem. **107**, 168–184 (2019). https://doi.org/10.1016/J.ENGANABOUND.2019.06.007
11. Dehghan, M., Shafieeabyaneh, N.: Local radial basis function-finite-difference method to simulate some models in the nonlinear wave phenomena: regularized long-wave and extended Fisher-

Kolmogorov equations. Eng. Comput. **37**, 1159–1179 (2021). https://doi.org/10.1007/s00366-019-00877-z
12. Eren, H.: Numerical study of unsteady interacting compressible jet flows using finite difference method for small Reynolds numbers. Appl. Math. Comput. **172**(2), 876–891 (2006). https://doi.org/10.1016/j.amc.2005.02.029
13. Erturk, E., Gökçöl, C.: Fourth-order compact formulation of Navier-Stokes equations and driven cavity flow at higher Reynolds numbers. Int. J. Numer. Methods Fluids **50**(4), 421–436 (2006). https://doi.org/10.1002/fld.1061
14. Fairweather, G., Mitchell, A.R.: A new computational procedure for A.D.I. methods. SIAM J. Numer. Anal. **4**(2), 163–170 (1967). https://doi.org/10.1137/0704016
15. Fletcher, C.A.J.: Generating exact solutions of the two-dimensional Burgers' equations. Int. J. Numer. Methods Fluids **3**(3), 213–216 (1983). https://doi.org/10.1002/fld.1650030302
16. Ghia, U., Ghia, K.N., Shin, C.T.: High-Re solutions for incompressible flow using the Navier-Stokes equations and a multigrid method. J. Comput. Phys. **48**(3), 387–411 (1982). https://doi.org/10.1016/0021-9991(82)90058-4
17. Guo, G., Lü, S.: Unconditional stability of alternating difference schemes with intrinsic parallelism for two-dimensional fourth-order diffusion equation. Comput. Math. Appl. **71**(10), 1944–1959 (2016). https://doi.org/10.1016/j.camwa.2016.03.004
18. He, D.: On the L^∞-norm convergence of a three-level linearly implicit finite difference method for the extended Fisher-Kolmogorov equation in both 1D and 2D. Comput. Math. Appl. **71**(12), 2594–2607 (2016). https://doi.org/10.1016/j.camwa.2016.04.026
19. Hirsh, R.S.: Higher order accurate difference solutions of fluid mechanics problems by a compact differencing technique. J. Comput. Phys. **19**, 90–109 (1975). https://doi.org/10.1016/0021-9991(75)90118-7
20. Ilati, M., Dehghan, M.: Direct local boundary integral equation method for numerical solution of extended Fisher-Kolmogorov equation. Eng. Comput. **34**, 203–213 (2018). https://doi.org/10.1007/s00366-017-0530-1
21. Johnston, H., Liu, J.G.: Finite difference schemes for incompressible flow based on local pressure boundary conditions. J. Comput. Phys. **180**, 120–154 (2002). https://doi.org/10.1006/jcph.2002.7079
22. Kalita, J.C., Dalal, D.C., Dass, A.K.: A class of higher order compact schemes for the unsteady two-dimensional convection-diffusion equation with variable convection coefficients. Int. J. Numer. Methods Fluids **38**(12), 1111–1131 (2002). https://doi.org/10.1002/fld.263
23. Kalogirou, A., Keaveny, E.E., Papageorgiou, D.T.: An in-depth numerical study of the two-dimensional Kuramoto-Sivashinsky equation. Proc. R. Soc. A **471**, 20140932 (2015). https://doi.org/10.1098/rspa.2014.0932
24. Karaa, S., Zhang, J.: High order ADI method for solving unsteady convection-diffusion problems. J. Comput. Phys. **198**, 1–9 (2004). https://doi.org/10.1016/j.jcp.2004.01.002
25. Kelly, C.T.: Iterative Methods for Linear and Nonlinear Equations. SIAM Publications, Philadelphia (1995). https://doi.org/10.1137/1.9781611970944
26. Khiari, N., Omrani, K.: Finite difference discretization of the extended Fisher-Kolmogorov equation in two dimensions. Comput. Math. Appl. **62**(11), 4151–4160 (2011). https://doi.org/10.1016/j.camwa.2011.09.065
27. Kuramoto, Y., Tsuzuki, T.: Persistent propagation of concentration waves in dissipative media far from thermal equilibrium. Prog. Theor. Phys. **55**(2), 356–369 (1976). https://doi.org/10.1143/PTP.55.356
28. Li, M., Tang, T., Fornberg, B.: A compact fourth-order finite difference scheme for the steady incompressible Navier-Stokes equations. Int. J. Numer. Methods Fluids **20**(10), 1137–1151 (1995). https://doi.org/10.1002/FLD.1650201003
29. Liu, F., Zhao, X., Liu, B.: Fourier pseudo-spectral method for the extended Fisher-Kolmogorov equation in two dimensions. Adv. Differ. Equations **2017**, 94 (2017). https://doi.org/10.1186/s13662-017-1154-x
30. Meitz, H.L., Fasel, H.F.: A compact-difference scheme for the Navier-Stokes equations in vorticity-velocity formulation. J. Comput. Phys. **157**, 371–403 (2000). https://doi.org/10.1006/jcph.1999.6387
31. Mittal, R.C., Kumar, S., Jiwari, R.: A cubic B-spline quasi-interpolation method for solving two-dimensional unsteady advection diffusion equations. Int. J. Numer. Methods Heat Fluid Flow **30**(9), 4281–4306 (2020). https://doi.org/10.1108/hff-07-2019-0597

32. Mittal, R.C., Tripathi, A.: Numerical solutions of two-dimensional unsteady convection-diffusion problems using modified bi-cubic B-spline finite elements. Int. J. Comput. Math. **94**, 1–21 (2017). https://doi.org/10.1080/00207160.2015.1085976
33. Mohanty, R.K., Jain, M.K.: High accuracy difference schemes for the system of two space nonlinear parabolic differential equations with mixed derivatives and variable coefficients. J. Comput. Appl. Math. **70**, 15–32 (1996). https://doi.org/10.1016/0377-0427(95)00135-2
34. Mohanty, R.K., Kaur, D.: High accuracy compact operator methods for two-dimensional fourth order nonlinear parabolic partial differential equations. Comput. Methods Appl. Math. **17**, 617–641 (2017). https://doi.org/10.1515/cmam-2016-0047
35. Mohanty, R.K., Setia, N.: A new high accuracy two-level implicit off-step discretization for the system of two space dimensional quasi-linear parabolic partial differential equations. Appl. Math. Comput. **219**(5), 2680–2697 (2012). https://doi.org/10.1016/j.amc.2012.08.100
36. Mohanty, R.K., Singh, S.: A new two-level implicit discretization of $O(k^2+kh^2+h^4)$ for the solution of singularly perturbed two-space dimensional non-linear parabolic equations. J. Comput. Appl. Math. **208**(2), 391–403 (2007). https://doi.org/10.1016/j.cam.2006.10.023
37. Mohanty, R.K., Kaur, D., Singh, S.: A class of two- and three-level implicit methods of order two in time and four in space based on half-step discretization for two-dimensional fourth order quasi-linear parabolic equations. Appl. Math. Comput. **352**, 68–87 (2019). https://doi.org/10.1016/j.amc.2019.01.050
38. Mohanty, R.K., Manchanda, G., Khan, A.: Operator compact exponential approximation for the solution of the system of 2D second order quasi-linear elliptic partial differential equations. Adv. Differ. Equations **2019**, 47 (2019). https://doi.org/10.1186/S13662-019-1968-9
39. Saray, B.N., Lakestani, M., Dehghan, M.: On the sparse multiscale representation of 2-D Burgers equations by an efficient algorithm based on multiwavelets. Numer. Methods Partial Differ. Equations **39**(3), 1938–1961 (2021). https://doi.org/10.1002/num.22795
40. Omrani, K.: Numerical methods and error analysis for the nonlinear Sivashinsky equation. Appl. Math. Comput. **189**, 949–962 (2007). https://doi.org/10.1016/j.amc.2006.11.169
41. Peaceman, D.W., Rachford, H.H., Jr.: The numerical solution of parabolic and elliptic differential equations. J. Soc. Ind. Appl. Math. **3**, 28–41 (1955). https://doi.org/10.1137/0103003
42. Pereira, J.M.C., Kobayashi, M.H., Pereira, J.C.F.: A fourth-order-accurate finite volume compact method for the incompressible Navier-Stokes solutions. J. Comput. Phys. **167**, 217–243 (2001). https://doi.org/10.1006/JCPH.2000.6673
43. Rohila, R., Mittal, R.C.: An efficient Bi-cubic B-spline ADI method for numerical solutions of two-dimensional unsteady advection diffusion equations. Int. J. Numer. Methods Heat Fluid Flow **28**(11), 2620–2649 (2018). https://doi.org/10.1108/HFF-12-2017-0511
44. Sivashinsky, G.I.: Instabilities, pattern-formation, and turbulence in flames. Ann. Rev. Fluid Mech. **15**, 179–199 (1983). https://doi.org/10.1146/ANNUREV.FL.15.010183.001143
45. Spotz, W.F., Carey, G.F.: High-order compact scheme for the steady stream-function vorticity equations. Int. J. Numer. Methods Eng. **38**(20), 3497–3512 (1995). https://doi.org/10.1002/NME.1620382008
46. Strikwerda, J.C.: High-order-accurate schemes for incompressible viscous flow. Int. J. Numer. Methods Fluids **24**(7), 715–734 (1997). https://doi.org/10.1002/(SICI)1097-0363(19970415)24:7<715::AID-FLD513>3.0.CO;2-E
47. Tafti, D.: Alternate formulations for the pressure equation Laplacian on a collocated grid for solving the unsteady incompressible Navier-Stokes equations. J. Comput. Phys. **116**, 143–153 (1995). https://doi.org/10.1006/JCPH.1995.1012
48. Weinan, E., Liu, J.G.: Essentially compact schemes for unsteady viscous incompressible flows. J. Comput. Phys. **126**, 122–138 (1996). https://doi.org/10.1006/jcph.1996.0125
49. Yanwen, M., Dexun, F., Kobayashi, T., Taniguchi, N.: Numerical solution of the incompressible Navier-Stokes equations with an upwind compact difference scheme. Int. J. Numer. Methods Fluids **30**(5), 509–521 (1999). https://doi.org/10.1002/(SICI)1097-0363(19990715)30:5<509::AID-FLD851>3.0.CO;2-E
50. Guozhen, Z.: Experiments on director waves in nematic liquid crystals. Phys. Rev. Lett. **49**(18), 1332–1335 (1982). https://doi.org/10.1103/PHYSREVLETT.49.1332
51. Başhan, A., Uçar, Y., Yağmurlu, N.M., Esen, A.: Numerical solutions for the fourth order Extended Fisher-Kolmogorov equation with high accuracy by differential quadrature method. Sigma J. Eng. Nat. Sci. **9**(3), 273–284 (2018). https://www.researchgate.net/publication/329529153

52. Başhan, A.: A numerical treatment of the coupled viscous Burgers' equation in the presence of very large Reynolds number. Phys. A **545**, 123755 (2020). https://doi.org/10.1016/j.physa.2019.123755
53. Uçar, Y., Yağmurlu, N.M., Başhan, A.: Numerical solutions and stability analysis of modified Burgers equation via modified cubic b-spline differential quadrature methods. Sigma J. Eng. Nat. Sci. **37**, 129–142 (2019). https://www.researchgate.net/publication/332031463
54. Wood, W.L.: An exact solution for Burgers' equation. Commun. Numer. Methods Eng. **22**(7), 797–798 (2006). https://doi.org/10.1002/cnm.850
55. Doss, L.J.T., Nandini, A.P.: A fourth-order H^1-Galerkin mixed finite element method for Kuramoto-Sivashinsky equation. Numer. Methods Partial Differ. Equations **35**(2), 445–477 (2019). https://doi.org/10.1002/num.22306
56. Mohanty, R.K., Manchanda, G., Khan, A.: Compact half step approximation in exponential form for 2D second order quasi-linear elliptic partial differential equations. J. Differ. Equations Appl. **25**(5), 716–749 (2019). https://doi.org/10.1080/10236198.2019.1624737
57. Mohanty, R.K., Sharma, D.: A new 2-level implicit high accuracy compact exponential approximation for the numerical solution of nonlinear fourth order Kuramoto-Sivashinsky and Fisher-Kolmogorov equations. J. Math. Chem. **62**, 973–1011 (2024). https://doi.org/10.1007/s10910-024-01577-w
58. Mohanty, R.K., Sharma, D.: A new 2-level compact off-step implicit method in exponential form for the solution of fourth order nonlinear parabolic equations. J. Math. Chem. **61**, 1165–1204 (2023). https://doi.org/10.1007/s10910-023-01451-1
59. Jain, M.K.: Numerical Solution of Differential Equations: Finite Difference and Finite Element Methods. New AGE International Publishers, 4th Edit., New Delhi (2018)
60. Dehghan, M., Mohammadi, V.: The boundary knot method for the solution of two-dimensional advection reaction-diffusion and Brusselator equations. Int. J. Numer. Methods Heat Fluid Flow **31**(1), 106–133 (2021). https://doi.org/10.1108/HFF-10-2019-0731
61. Mohammadi, V., Dehghan, M.: A POD-RBF-FD scheme for simulating chemotaxis models on surfaces. Eng. Anal. Boundary Elem. **143**, 316–330 (2022). https://doi.org/10.1016/j.enganabound.2022.06.024